Eötvös Loránd University
Corvinus University of Budapest

Variance Derivatives and the Effect of Jumps on Them

MSc Thesis

Zsófia Tagscherer

MSc in Actuarial and Financial Mathematics
Faculty of Quantitative Finance

Supervisors:

Zsófia Iványi
Gábor Molnár-Sáska

Budapest, 2018

Acknowledgements

I would like to express my gratitude to my supervisor, Zsófia Iványi for her time, useful advices, patience and for the many consultations. Many thanks to Gábor Molnár-Sáska for the topic suggestion. Finally, I would like to thank my family for ensuring such a supportive and calm environment.

Contents

Chapter 1

Introduction

Volatility is the most popular statistical measure by which we can describe the instability of the market, it expresses the variation of an underlying's price over time measured by the standard deviation of the asset's returns. Therefore, it is an appropriate measure by which the riskiness of any traded product can be quantified. Volatility is usually expressed in annual terms in order to be comparable. We can distinguish different types of volatilities: *historical* or *realized volatility* is a measure which depends on the past market prices of the asset. On the other hand, *implied volatility* refers to the expectation of future realized volatility by market participants. It is obtained from currently available market prices of such derivatives on the underlying which affected by the volatility.

Probably, the most important motivation for trading volatility is the desire to hedge risks caused by the instability of the underlying's price. In order to create a vega-neutral position (i.e. eliminate the risk of volatility), the most effective way is to take pure[1] exposure to volatility in the opposite direction.
Many investors also want to trade volatility for speculating purposes. For instance, one can think the actual implied volatility divers from the "fair" one, so they wish to realize the hypothetical difference. Others can have expectations about the variation of the market over the following period.
To accomplish the previously mentioned goals (among many others), the best way is to trade a volatility based derivative. One purpose of this thesis to present some derivatives by which pure exposure can be taken to the volatility (or its square, the variance) of the underlying's price. Although, derivatives on realized volatility are also an interesting topic but in this thesis I decided to analyze the products based on realized variance. An other aim is to study the pricing (and, thereby in some cases the hedging) of the selected derivatives and the impact of jumps on them.

[1]Volatility exposures can be hedged by trading options as well but owing an option means being exposed not only the vega risk but also to the risk of the movements in the asset's price.

The structure of this thesis is the following: in the second chapter I present some theoretical background which are referred in many cases throughout the thesis. Two models (the Heston and the Bates stochastic volatility models) and a method (Monte Carlo Simulation) - used for pricing purposes during the whole implementation - are also introduced later in chapter 2.

In the beginning of chapter 3 the structure of variance swaps are discussed. Then I present the model independent replicating strategy with some numerical tests regarding its limitations. Finally, the fair prices are derived under the two selected models.

In chapter 4, other variance and volatility related products are presented. Some of them are just briefly mentioned but the ones with greater significance regarding this thesis are discussed is more details. Although volatility dependent products are also commonly traded, the main focus of this thesis was placed on variance based derivatives: I priced variance, gamma, corridor and capped variance swaps.

Chapter 5 contains the numerical and experimental results. Firstly, the calibrations of the two selected model to real market $S\&P500$-data are presented. Also, some stability tests were performed in order to examine the reliability of the calibrations. Then, a specific discretization and simulation method is introduced which were essential for pricing in many cases. After the introduction of the necessary preparations, an important part of this thesis, the results are presented. In the first subsection, I determined the prices of variance and gamma swaps by their replicating portfolio using real market data. Later in this section, the prices depend on the selected models' parameters. Simulation results are compared between the models and the different derivatives. After the basic pricing of such derivatives, I examined the impact of jumps. A relevant motivation of this investigation is to get some foreknowledge about how much error is made by - for instance - hedging a derivative by its replicating portfolio if the market cannot be described appropriately under a continuous model. The effects of jumps on the prices of variance, gamma and capped variance swaps were tested by the jump parameters. Finally, I checked how the variance swap's price is affected by caps and (in an other case) by corridors under the two different models along with their calibrated parameters.

Chapter 6 summarizes the results.

Chapter 2

Applied models and tools

In this chapter, I am going to present the most essential part of stochastic calculus regarding this thesis, a popular tool which is adequate for pricing and two models under which the prices of the selected derivatives are determined.

Throughout this thesis work, I used these two models for modelling the underlying asset price process. Since the Black-Scholes-Merton model assumes constant volatility - among other restrictions - it is not suitable for pricing products which payoffs depend on the realized variance/volatility of the underlying asset's return. For this reason the main aspect of model selection was the structure of the variance: it should be handled as a stochastic process. The first model is Heston's (1993) stochastic volatility model which is a frequently used, continuous model, i.e. there isn't any jump neither in the variance nor the asset's price processes. The second one - also a popular model - is an extension of Heston's model with jumps in the underlying price process proposed by Bates (1996).

2.1 Stochastic calculus

The following definition and theorem are based on Klebaner's book, [10].

Definition 2.1 (Ito drift-diffusion process)**.** An $X(t)$ *Ito drift-diffusion process* has the form

$$X(t) = X(0) + \int_0^t \mu(s, X_s)ds + \int_0^t \sigma(s, X_s)dW_s, \quad 0 \leq t \leq T$$

where $X(0)$ is $\mathcal{F}_0$-measurable, processes $\mu(t, X_t)$ and $\sigma(t, X_t)$ are $\mathcal{F}_t$-adapted, such that $\int_0^T |\mu(t, X_t)|dt < \infty$ and $\int_0^T \sigma^2(t, X_t)dt < \infty$.
X(t) has the stochastic differential on $[0, T]$:

$$dX(t) = \mu(t, X_t)\ dt + \sigma(t, X_t)\ dW_t, \quad 0 \leq t \leq T. \tag{2.1}$$

Theorem 2.2 (Ito's formula for $f(X_t)$)**.** *Let X_t be an Ito process with (2.1) stochastic differential on $[0,T]$. If f is twice continuously differentiable function ($f \in C^2$), then the stochastic differential of the process $Y(t) = f(X_t)$ exists and it's given by*

$$\begin{aligned} df(X_t) &= f'(X_t)dX_t + \frac{1}{2}f''(X_t)d[X]_t \\ &= \left(f'(X_t)\mu(t,X_t) + \frac{1}{2}f''(X_t)\sigma^2(t,X_t)\right)dt + f'(X_t)\sigma(t,X_t)dW_t, \end{aligned} \tag{2.2}$$

or in integral form

$$f(X_t) = f(X_0) + \int_0^t \left(f'(X_s)\mu(s,X_s) + \frac{1}{2}f''(X_s)\sigma^2(s,X_s)\right)ds + \int_0^t f'(X_s)\sigma(s,X_s)dW_s$$

It follows from the definition that $f(X_t)$ is also an Ito process.

2.2 Monte Carlo simulation

Monte Carlo simulation is a popular tool which can be used for pricing purposes. The essence of this technique is to model the uncertainty by gathering possible outcomes. If we suppose that a specified framework (e.g. Black-Scholes-Merton/Heston/Bates model) can describe the market appropriately, we can simulate the underlying price process by the assumed dynamics under the selected model. Using the simulated future prices, many future payoffs (functions of the stochastic future prices) can be calculated. Discounting these future payoffs to time-0, and determining the average value along the paths, we obtain the ($t = 0$) price - present value - of the selected derivative. More stable result can be achieved by increasing the number of paths.

2.3 Heston's model

Under the Heston stochastic volatility model, (based on Heston's publication, [13]) the price of the underlying asset and the corresponding variance process are modelled with the following differential equations:

$$\frac{dS_t}{S_t} = \mu\ dt + \ \sqrt{v_t}\ dW_t^S, \tag{2.3}$$

$$dv_t = \kappa\ (\bar{v} - v_t)\ dt + \sigma_v\sqrt{v_t}\ dW_t^v, \tag{2.4}$$

$$Cov\big(dW_t^S, dW_t^v\big) = \rho\ dt.$$

Here, S_t denotes the price of the underlying asset at time t, v_t is the instantaneous variance, μ is the expected return on the underlying asset, κ is the speed of mean reversion, $\bar{v}$ is the long-term variance and σ_v is the volatility of volatility. W_t^S and W_t^v are two correlated standard Brownian motions with ρ correlation coefficient.
In order to make sure the variance process is not negative for any time t, the parameters must satisfy the so called Feller-condition:

$$2\kappa\bar{v} > \sigma_v^2.$$

It is important that this proposition is only valid under continuous time. As we discretize the variance process, it could become negative which need to be handled.

2.3.1 Properties of the Heston model

An important property of Heston's model is that the variance process is mean-reverting. From market data, the same feature can be observed for realized variance in many cases. An other attractive trait of this model is the existence of a semi-closed formula for European options' price.
Beside the previously mentioned advantages, it has drawbacks as well. One weakness of this model is that the calibrated parameters usually unable to fulfill the Feller-condition. A different empirical issue, especially for shorter maturities that the model implied volatilities are incapable of giving back the market implied smile.

Under the Heston model the variance is modelled as a CIR-process. Cox, Ingersoll and Ross derived the probability distribution of the variance process at time t on condition of its value at time s, where $s < t$. According to their publication, [7], the conditional probability distribution of the random variable, $2c_t v_t$ depending on the value of v_s is non-central chi-squared, where the non-centrality parameter is $2c_t v_s e^{-\kappa[t-s]}$, the degree of freedom is $d = 2\kappa\bar{v}/\sigma_v$ and

$$c_t = \frac{2\kappa}{\sigma_v^2\left(1 - e^{-\kappa[t-s]}\right)}.$$

Applying this feature, the conditional expectation and variance of v_t on condition of the value of v_s can be expressed as

$$E\left[v_t|v_s\right] = (v_s - \bar{v})e^{-\kappa[t-s]} + \bar{v}, \tag{2.5}$$

$$D^2\left[v_t|v_s\right] = \frac{\sigma_v^2}{\kappa} v_s \left(e^{-\kappa[t-s]} - e^{-2\kappa[t-s]}\right) + \frac{\bar{v}\sigma_v^2}{2\kappa}\left(1 - e^{-\kappa[t-s]}\right)^2. \tag{2.6}$$

2.4 The Bates model

This model - proposed by Bates - is a combination of Heston's stochastic volatility and Merton's jump diffusion model. The stochastic differential equations under the Bates model are[1]

$$\frac{dS_t}{S_t} = \mu\ dt + \ \sqrt{v_t}\ dW_t^S + dJ_t, \tag{2.7}$$

$$dv_t = \kappa\ (\bar{v} - v_t)\ dt + \sigma_v \sqrt{v_t}\ dW_t^v, \tag{2.8}$$

$$Cov\big(dW_t^S, dW_t^v\big) = \rho\ dt,$$

with notation $J_t = \sum_{i=1}^{N_t}(Y_i - 1)$, where N_t is a Poisson-process with λ jump intensity rate and $Y_i \sim LN(a, b^2)$ is the relative jump size. An assumption of this model is that the Poisson process (N_t) and the relative jump size (Y_i) are independent of one other and of the Brownian motions $(W_t^S,\ W_t^v)$.

2.4.1 Properties of the Bates model

The model proposed by Bates in [2] is suitable for modelling a flexible distribution structure. This model can handle the skew observed on the market more efficiently than the Heston model. Under Bates' model the implied skew can arise from two sources. Firstly, similarly to the Heston model, the skew is caused by the correlation, ρ between the price and variance processes. The other origin of the implied skew is the existence of non-zero jumps.
The distribution of the underlying price implied by the Bates model can reproduce an other stylized fact, the excess kurtosis. It is affected by the volatility of volatility, σ_v like in Heston's model and the jump component.
Likewise to the Heston model, a semi-closed formula for European option prices is derived by which a faster calibration can be accomplished.

The conditional distribution of the variance process depending on an earlier value of the process and therefore, the conditional expectation and variance are the same as in the Heston model's case since the variance processes are identical.

[1] with notations as in [3]

Chapter 3

Variance Swaps

Variance swaps are financial derivatives on future realized variance. They allow investors to bet on the future level of realized variance without taking exposure to the underlying asset's price. These instruments are generally over-the-counter (OTC) derivatives but there are similar products which are traded on exchanges as well. The payoff function of such a contract at maturity, T is the difference between the future realized variance (over the life of the contract) and the fair variance strike times a predefined constant called notional:

$$X(T) = (\sigma_R^2 - K_{var}) \times N.$$

K_{var} is set at inception to make the initial value of the contract equals to zero like in the case of vanilla swaps. The realized variance over $[0, T]$ time horizon, σ_R^2 is expressed in annual term and defined below. At maturity, if $\sigma_R^2 > K_{var}$, then the investor who owes a *long position* on a variance swap receives the notional, N after every surplus variance points by which the fair strike is exceeded by the realized variance. In the case of $\sigma_R^2 < K_{var}$, the investor needs to pay this amount to his/her counterparty. The payoff of a *short position* is the negation of the long position's.

The realized variance over $[0, T]$ can be expressed in the discrete-time as,

$$\sigma_R^2 = \frac{AF}{M} \cdot \sum_{i=1}^{M} \ln\left(\frac{S_i}{S_{i-1}}\right)^2, \qquad \text{or} \qquad \sigma_R^2 = \frac{AF}{M} \cdot \sum_{i=1}^{M} \left(\frac{S_i - S_{i-1}}{S_{i-1}}\right)^2 \tag{3.1}$$

and in continuous-time as well:

$$\sigma_R^2 = \frac{1}{T} \int_0^T \sigma_t^2 \, dt,$$

where AF stands for the annualization factor and M is the number of sub-intervals by which $[0, T]$ time horizon is divided. The first expression in (3.1) is called log-realized variance and in this thesis it is considered as the default choice.

For an investor, trading variance swaps can be attractive for many reasons. He/She can for example hedge his/her variance exposure or speculate on the future level of variance. Although, these actions can be done by trading options as well, using a variance swap is more effective. It is because, pure exposure to variance is accessible without the need of delta-hedging via variance swaps. An also very important property of variance swaps is the vega-neutrality. This means that small movements in the implied volatility doesn't change the variance swap's price. Whereas, considering a delta-hedged option, its price is sensitive to the changes in implied volatility.
Generally, we can classify the market participants by their intentions to three groups. There are investors who want to bet directly on the future level of variance to express their views. An other group of participants whose purpose is to trade the spread between realized and implied variance. Finally, there are clients who use the variance swaps for hedging their volatility exposures.

3.1 Model-independent replication

Certainly, a prosperous feature of a variance swap is the fact that it can be replicated by a portfolio of plain vanilla call and put options. Since we can observe option prices on the market, this replication can be done in a model-independent way. In theory, the value of this portfolio must coincides with the theoretical value of the variance swap. However, due to the fact that we can not observe option prices for all strikes from 0 to ∞, in practice this replication is never perfect. The rest of this section presents the methodology of [9].
Although it is a model-free replication we still have some assumptions. Firstly, the dynamic of the underlying price process needs to be continuous, i.e. jumps are not allowed. An other supposition refers to the interest rate process, which is expected to be deterministic. For simplicity, lets assume that the underlying does not pay dividends and the risk-free interest rate, r is constant (these are not necessary assumptions for the validity of replication). Under these hypothesis the price evolution is defined by the next equation:

$$\frac{dS_t}{S_t} = \mu(t, \dots)dt + \sigma(t, \dots)dW_t, \tag{3.2}$$

where dW_t is an increment of a standard Brownian motion. In the continuous world, the annualized, realized variance from time 0 until T should be expressed as an integral of

the variance process over the $[0, T]$ interval

$$V = \frac{1}{T}\int_0^T \sigma^2(t, \dots)dt. \tag{3.3}$$

To determine the fair strike value of the variance swap, we should price it as a simple forward contract, so that

$$F = E[e^{-rT}(V - K_{var})].$$

After some simplification and taking into account the fact that our goal is to set the present value to 0, we get

$$\begin{aligned} K_{var} &= E[V] \\ &= \frac{1}{T}E\left[\int_0^T \sigma^2(t, \dots)dt\right]. \end{aligned} \tag{3.4}$$

Unfortunately, the variance process, $\sigma^2(t, \dots)$ is usually not known, cannot be observed. For this reason it is not possible to compute the exact value of the expectation. It can be approximated by using a Monte-Carlo simulation but this procedure depends on a selected model.

In order to obtain the replicating portfolio, firstly, we need to determine the dynamic of the logarithm of the price process, $d\ln(S_t)$. By applying Ito's lemma, we get

$$d\ln(S_t) = \left(\mu(t, \dots) - \frac{1}{2}\sigma^2(t, \dots)\right)dt + \sigma dW_t. \tag{3.5}$$

We should notice that after substracting (3.5) from (3.2), what remains is

$$\frac{dS_t}{S_t} - d\ln(S_t) = \frac{1}{2}\sigma^2(t, \dots)dt.$$

After multiplying the whole equation by 2, it can be inserted into (3.4), so that

$$\begin{aligned} K_{var} &= \frac{2}{T}E\left[\int_0^T \frac{dS_t}{S_t} - d\ln(S_t)\right] \\ &= \frac{2}{T}E\left[\int_0^T \frac{dS_t}{S_t} - \ln\frac{S_T}{S_0}\right]. \end{aligned} \tag{3.6}$$

Here, we should keep in mind the fact that the risk-neutral framework is applicable for pricing, therefore

$$\frac{dS_t}{S_t} = r\ dt + \sigma(t, \dots)dW_t^*$$

holds true for the price evolution. Integrating it over the $[0, T]$ interval, then taking its expected value under the risk-neutral measure, we obtain

$$E^* \left[\int_0^T \frac{dS_t}{S_t} \right] = rT. \tag{3.7}$$

Note that, $E^*[dW_t] = 0$ (a property of the Brownian motion) was used. The second part under the expectation in (3.6) corresponds the payoff function of a log-contract at maturity. Even though in such that form it is not an actively traded derivative, it can be split into two parts:

$$\ln \frac{S_T}{S_0} = \ln \frac{S_T}{S*} + \ln \frac{S*}{S_0}, \tag{3.8}$$

where $S*$ should be chosen as the boundary strike between Out of The Money put and call options. Due to $S*$ is a predefined constant, $\ln(S*/S_0)$ is also a constant, so its expected value will be itself.

It has been shown in several publications, e.g. [5] that any twice differentiable payoff function (or any smooth function of the time T future price), $f(F_T)$ can be expressed in terms of a static positions in vanilla put and call options:

$$\begin{aligned} f(F_T) = f(\kappa) + f'(\kappa) \left[(F_T - \kappa)^+ - (\kappa - F_T)^+ \right] \\ + \int_0^\kappa f''(K)(K - F_T)^+ dK \\ + \int_\kappa^\infty f''(K)(F_T - K)^+ dK. \end{aligned} \tag{3.9}$$

Applying eq. (3.9) to the log-payoff function, $f(S_T) = -\ln \frac{S_T}{S*}$, with boundary $\kappa = S*$ we get a replication portfolio - as in [9] - of the first part of eq. (3.8), in terms of a forward contract and different put and call options. More precisely, the following decomposition holds for all future S_T:

$$\begin{aligned} -\ln \frac{S_T}{S*} = & -\frac{S_T - S*}{S*} \\ & + \int_0^{S*} \frac{1}{K^2}(K - S_T)^+ dK \\ & + \int_{S*}^\infty \frac{1}{K^2}(S_T - K)^+ dK. \end{aligned} \tag{3.10}$$

The first component is equivalent to $(1/S*)$ short forward position with strike rate $K = S*$. The other two components are long positions in portfolios of put and call options, respectively. The options are weighted inversely proportional to the square of the strikes, where the strikes vary from 0 to $S*$ in case of put options and from $S*$ to ∞ regarding the portfolio of call options.

Substituting (3.7), (3.8) and (3.10) to (3.6) we get the following equation for the fair

variance strike

$$K_{var} = \frac{2}{T}\left[rT - \left(\frac{S0}{S*}\, e^{rT} - 1\right) - \ln\frac{S*}{S0}\right] + \frac{2}{T}\, e^{rT}\left[\int_0^{S*} \frac{1}{K^2}P(K)dK + \int_{S*}^{\infty} \frac{1}{K^2}C(K)dK\right]. \tag{3.11}$$

In the previous equation, on condition that K is the strike, $C(K)$ and $P(K)$ stand for the fair prices of call and put options, respectively.
It is worth to note that the fair strike of a variance swap can be expressed in a simpler way. If we set $S*$ to the fair forward price ($S0 \cdot e^{rT}$), only the last parts of eq. (3.11) remain, therefore, K_{var} is defined by a pure portfolio of call and put options:

$$K_{var} = \frac{2}{T}\, e^{rT}\left[\int_0^{S*} \frac{1}{K^2}P(K)dK + \int_{S*}^{\infty} \frac{1}{K^2}C(K)dK\right].$$

3.1.1 Limitations of the model-free replication

Although, in theory the variance swaps can be perfectly replicated by a portfolio of options and a forward position, in practice this portfolio just approximates the variance swap. This is a consequence of the limited strike range with which options are traded. In order to obtain the perfectly replicating portfolio, according to eq. (3.11) put option prices for all strike K, from 0 to $S*$ and call option prices for $\forall K \in [S*, \infty]$ are required. On the contrary, the number of available strikes are limited. As the length of the strike range increases and the size of the steps between the strikes decreases, the value of the replicating portfolio is getting closer to the theoretical value of the variance swap. In order to illustrate this convergence, tables 3.1 and 3.2 below summarize the results of an example. Here, we supposed that the market can be represented properly under the Black-Scholes (B-S) world, so that the B-S formula can be used for computing the option prices. The risk-free interest rate and dividend are fixed at zero, $r = 0$ and $d = 0$, the spot price of the underlying at inception, $S_0 = 100$ and the constant volatility is $\sigma = 20\%$.

ΔK	10	5	1	0.1	0.01
$T = 0.25$	$(28.03)^2$	$(24.00)^2$	$(20.79)^2$	$(20.07)^2$	$(20.00)^2$
$T = 0.5$	$(25.66)^2$	$(22.82)^2$	$(20.56)^2$	$(20.05)^2$	$(20.00)^2$
$T = 1$	$(23.99)^2$	$(21.99)^2$	$(20.39)^2$	$(20.03)^2$	$(20.00)^2$

TABLE 3.1: Convergence to the fair variance strike as $\Delta K \to 0$.

In table 3.1 the studied strike range is fairly wide, $50\% - 200\%$ of the ATM forward price to have enough sub-intervals even in the case of $\Delta K = 10$. The estimated fair variance strikes are calculated by eq. (3.11) using sums in place of integrals and expressed in

percentage form. We can see that as the spacing between the strikes decreases and therefore, the number of options in the replicating portfolio increases, the estimated fair variance strike converges to its theoretical value. An other conclusion connects to the maturity: the sooner the expiration of the variance swap is, the higher the discrepancies between the theoretical and empirical values of the fair variance strikes are.

Strike range	$90\% - 110\%$	$50\% - 150\%$	$0\% - 200\%$
$T = 0.25$	$(18.54)^2$	$(20.07)^2$	$(20.07)^2$
$T = 0.5$	$(17.07)^2$	$(20.05)^2$	$(20.05)^2$
$T = 1$	$(15.33)^2$	$(19.99)^2$	$(20.03)^2$
$T = 2$	$(13.50)^2$	$(19.79)^2$	$(20.01)^2$

TABLE 3.2: Convergence to the fair variance strike as the range of K is broadening.

In table 3.2, the calculations are done similarly, with $\Delta K = 0.1$. The considered strike ranges are expressed in percentage of the forward price and the obtained variance strikes are in squared-percentage. From the results we can see that for a fixed maturity, as the strike range increases, the captured variance increases as well. On the other hand, for a fixed strike range, the sooner the expiration is, the higher the variance strike is. It follows that for replicating a variance swap with longer maturity, a wider strike range and/or smaller step size between strikes should be considered.

An other source of the misestimation of the variance swap's value by its replicating portfolio can be the possible jumps in the underlying price process. Notwithstanding that the price dynamic is assumed to be diffusive, it is not always materialized. What is more, in many cases, we can achieve better fits to market with models under which jumps are allowed. The authors of [9] show the impact of only one jump in the underlying price assuming the options are traded with all strikes, i.e. option prices can be observed for all K. For this derivation, let's suppose that $\Delta S_j = S_j - S_{j-1}$, $\sigma_R = \frac{1}{T}\sum \Delta S_j/S_{j-1}$ and if a jump happens at time t_i, then $S_i = S_{i-1}(1 - J)$. If we try to capture the realized variance by a log-contract, i.e.

$$V(T) = \frac{2}{T}\left(\sum_{j=1}^{T}\frac{\Delta S_j}{S_{j-1}} - \ln\frac{S_T}{S_0}\right),$$

the contribution of a single jump is

$$\frac{2}{T}\left(\frac{\Delta S_i}{S_{i-1}} - \ln\frac{S_i}{S_{i-1}}\right) = \frac{2}{T}[1 - J - \ln(1 - J)].$$

On the other hand, the exact contribution of one jump to the realized variance is

$$\frac{1}{T}\left(\frac{\Delta S_i}{S_{i-1}}\right)^2 = \frac{J^2}{T}.$$

The difference appears in the P&L of a portfolio of the realized variance, σ_R and a log-contract, where the directions of the exposures are opposite. After expanding the logarithm function around J, the remaining jump contribution in the P&L is

$$P\&L_{jump} = \frac{2}{3}\frac{J^3}{T} + \dots$$

Therefore, the impact of a single jump in the underlying price process to the P&L of a variance hedging strategy can be approximated by a cubic function.

3.2 Fair strike under the Heston model

In the continuous time horizon we can calculate the expected future realized variance only if we know the dynamic of the variance. Under the Heston model, the evolution of the variance process is defined by equation (2.4). Therefore, we can calculate the fair strike of a continuously sampled variance swap under the Heston dynamics.

As it is shown in section 2.3.1, the conditional expected value of the variance at t on condition of v_0 equals to:

$$E\big[v_t|v_0\big] = (v_0 - \bar{v})e^{-\kappa t} + \bar{v}.$$

According to equation (3.4) we get the fair variance strike as in [3]:

$$\begin{aligned} K_{var}^{Hest} &= \frac{1}{T}E\left[\int_0^T v_t dt \;\middle|\; v_0\right] \\ &= \frac{1}{T}\int_0^T E\big[v_t|v_0\big]\; dt \\ &= \frac{1}{T}\left[(v_0 - \bar{v})\frac{1 - e^{-\kappa T}}{\kappa} + \bar{v}T\right] \\ &= (v_0 - \bar{v})\frac{1 - e^{-\kappa T}}{\kappa T} + \bar{v}. \end{aligned} \tag{3.12}$$

Here, the order of taking the expectation and integrating can be exchanged due to Fubini's theorem.

3.3 Fair strike under the Bates model

Just like in the case of Heston model the fair variance strike for a variance swap can be computed under the Bates model. Although the variance processes are identical in these models, the realized variance of the underlying price over the life of the contract are not the same because of the jumps' contribution.

The future realized variance (based on [3]) over interval $[0, T]$ is:

$$V = \frac{1}{T}\int_0^T v_t \; dt + \frac{1}{T}\sum_{i=1}^{N_T}(\ln Y_i)^2,$$

where the second part is added due to N_T jumps in $[0, T]$. Taking the expected value of this amount we get the fair variance strike as

$$\begin{aligned} K_{var} &= E\left[V\right] \\ &= (v_0 - \bar{v})\frac{1 - e^{-\kappa T}}{\kappa T} + \bar{v} + \frac{1}{T} \cdot E\left[\sum_{i=1}^{N_T}(\ln Y_i)^2\right]. \end{aligned}$$

Because of the log-relative jump sizes, $(\ln Y_i)\ \forall\ i$ are *i.i.d.* and independent of the Poisson process, N_T as well

$$E\left[\sum_{i=1}^{N_T}(\ln Y_i)^2\right] = E\left[N_T\right] \cdot E\left[(\ln Y_i)^2\right]$$

equation holds true. Therefore, considering the distribution of $\ln Y_i \sim N(a, b^2)$ and using the well-known relationship between the expected value and the variance, $D^2[X] = E[X^2] - E^2[X]$, the fair variance strike under the Bates model is obtained in the form of

$$K_{var}^{Bates} = K_{var}^{Hest} + \lambda \cdot (a^2 + b^2), \tag{3.13}$$

which is the fair variance under the Heston model plus an extra element caused by the jumps.

Chapter 4

Other derivatives on variance

In this chapter I'm going to present some other financial derivatives on future realized variance/volatility. After a brief summary of the different types, a few selected product will be explained in more details.

Many different products exist by which an investor can take pure exposure to realized variance or volatility depending on their purpose. The most common derivative types on variance/volatility are the following[1]:

- variance/volatility swaps
- capped/floored variance/volatility swaps
- weighted variance swaps
- options on realized variance/volatility
- volatility index (VIX) options
- volatility index (VIX) futures

The first four examples are OTC derivatives. These are not standardized, the details of such contracts are fixed trade by trade. In contrast, the last two are traded on Chicago Board Options Exchange (CBOE) with standardized features like in case of other financial products traded on exchanges.

Based on the type of the weights in a weighted variance swap, we can specify several contracts, for example gamma swaps, corridor or conditional swaps or even the "simple" variance swap with weights, $w_i = 1 \ \forall i$.

[1]The list is not complete, other variance/volatility based derivatives exist as well.

4.1 Volatility Swaps

Volatility swaps are derivative contracts on future realized volatility, σ_R. Similarly to the structure of variance swaps, at maturity, T the investor receives (or pays) N^2 times the difference between the realized volatility over the life of the contract and the predefined, fair volatility strike, K_{vol}. The payoff function can be expressed in the form of

$$X(T) = (\sigma_R \ - K_{vol}) \times N.$$

Likewise to the fair variance strike, K_{vol} is fixed at inception to make the present value zero and both σ_R and K_{vol} are expressed in annual terms. Since the realized volatility is the square-root of realized variance the discrete-time formula for σ_R:

$$\sigma_R = \sqrt{\frac{AF}{M} \cdot \sum_{i=1}^{M} \ln\left(\frac{S_i}{S_{i-1}}\right)^2},$$

where AF is the annualization factor and M is the number of intervals by which $[0, T]$ is partitioned.

The most essential difference between variance and volatility swaps is related to their valuation and hedging. As it was mentioned in section 3.1, the fair variance strike of a variance swap can be obtained by valuing a replicating portfolio consists of options and a forward position. On the contrary, a similar portfolio cannot be specified for the fair volatility strike, therefore the pricing but more importantly the hedging of a volatility swap is more challenging. Why variance swaps are the replicable products instead of volatility swaps? The answer for this question arises from the profit and loss (P&L) distribution of a delta-hedged option - it is a linear function of the realized variance and not the realized volatility. It follows that, variance appears naturally by hedging options which is crucial for risk management purposes.

4.2 Capped/Floored Variance Swaps

A variance swap is generally written on an underlying asset which can be an index or a single stock. If the underlying is a stock, the issuer of the variance derivative may suffer an "unlimited" loss due to a potential huge fall in the underlying price. To avoid this and make these products more appealing and therefore more liquid, it is a common practice to write capped variance swaps on single name stocks. On the other hand, in the case of variance swaps written on indices, caps are not essential since a large decrease in one

[2] N denotes the notional amount of the contract.

stock's price does not affect the index's volatility remarkably.
The payoff function of a *capped variance swap* at maturity, T

$$X(T) = \left(\min\left[\sigma_R^2\ , C\right] - K_{var}\right) \times N,$$

where C denotes the cap, σ_R^2 is the realized variance over $[0, T]$ expressed in annual terms, K_{var} and N represent the fair strike and the notional, respectively. Caps are frequently fixed at 2.5 times the initial fair strike - according to [15] or [14] - which is a market convention but other caps can be determined as well.

Analogously, we can express the payoff of a *floored variance swap*, with floor F as

$$X(T) = \left(\max\left[\sigma_R^2\ , F\right] - K_{var}\right) \times N.$$

Equivalently, volatility swaps can be - and those that are written on single name equities, usually are - capped and floored as well.

4.3 Gamma Swaps

A special kind of variance swaps are *Gamma Swaps*. Their payoff at maturity, T depend on the periodically weighted realized variance over the life of the contracts. The weights are defined by the ratio of the actual spot price in the corresponding period and the initial price of the underlying.

$$X_{Gamma}(T) = (Gamma - K_{Gamma}) \times N,$$

where K_{Gamma} is the fair strike, N is the notional amount and AF stands for the annualization factor in the definition of *Gamma*:

$$Gamma = \begin{cases} \frac{AF}{M} \cdot \sum_{i=1}^{M} \left[\ln\left(\frac{S_i}{S_{i-1}}\right)^2 \cdot \frac{S_i}{S_0}\right] & \text{, in discrete-time} \\ \frac{1}{T}\int_0^T \sigma_t^2 \frac{S_t}{S_0}\, dt & \text{, in continuous-time.} \end{cases}$$

Dispersion trading means the exploitation of the well-known fact that difference between implied and realized volatility of index options is greater than this amount considering single-name stock options. By a static portfolio of gamma swaps, dispersion can be implemented, therefore such products are commonly used for this purpose.
An other popular application of gamma swaps is to trade the implied volatility skew.
Moreover, these products can be used if someone wants to trade the variance of a single

stock without cap - which is frequently attached to variance swaps written on a single stock - since the structure of gamma swaps does not require any.

While variance swaps' gamma exposures are insensitive to the level of the underlying asset (they have constant "cash" gamma), gamma swaps are designed to have linear gamma exposure. This means that the gamma exposure of gamma swaps are constant in terms of shares (i.e. gamma swaps have constant "share" gamma). This trait makes dispersion trading easier with gamma swaps than with variance swaps.

Many different methods exist for pricing such products. For example, gamma swaps admit model-free replication - it is shown in greater details in the following subsection.
Zheng and Kwon derived a closed-form pricing formula in [20] for discretely sampled gamma swaps under a stochastic volatility model with simultaneous jumps in the underlying price and variance processes. Their method relies on the solvability of the joint moment generating function of the log-price and the variance processes. They also determine a closed pricing formula for continuously sampled gamma swaps as the limit of the discretely sampled gamma swaps' pricing formula as the difference between observation days tends to zero.
Yuen, Zheng and Kwon priced discretely sampled gamma swaps under the 3/2 Stochastic Volatility Model. In their publication, [18] they used the two-step PIDE[3] approach for determining a formula for the fair strike of discretely sampled gamma swaps.
In [19], the authors introduce a new method to determine the discretely sampled fair gamma strike. They use multinomial trees to approximate different stochastic volatility models - for instance the Heston model or the Hull-White model. Then the fair strike is obtained by the decomposition of the payoff structure into nested conditional expectations.
Crosby and Davis - in [8] - derive exact formulas for both the discretely and continuously monitored fair strike of gamma swaps. They assume throughout their methodology that the log-price is driven by time-changed Lévy processes. The fair price formulas are defined by the characteristic function of the log-price process and its derivatives.

4.3.1 Model-free replication of Gamma Swaps

Likewise to the case of variance swaps, Carr and Madan's methodology, [5] can be applied to the valuation of gamma swaps as well. It follows that - under some assumptions - a continuously sampled gamma swap also has model-independent replication strategy which initial price will be the fair strike of the gamma swap, K_{Gamma}.

[3]Partial Integro-Differential Equation

Let's suppose that a future market of the risky asset exists and European options written on this risky underlying can be traded for all strikes. Moreover, we assume that the dynamic of the underlying price process is continuous, and for simplicity let's assume that the risk-free interest rate is zero and the underlying does not pay dividend $(r, d = 0)$. On the one part, by applying Ito's lemma, (2.2) to the payoff function

$$f(S_T) = \frac{S_T}{S_0} \ln\left(\frac{S_T}{S_0}\right) - \frac{S_T}{S_0} + 1 \tag{4.1}$$

we obtain

$$\frac{1}{2}\int_0^T \frac{S_t}{S_0}\sigma_t^2 dt = \frac{S_T}{S_0} \ln\left(\frac{S_T}{S_0}\right) - \frac{S_T}{S_0} + 1 - \frac{1}{S_0}\int_0^T \ln\left(\frac{S_t}{S_0}\right) dS_t \tag{4.2}$$

from which (the continuous) *Gamma* can be expressed by multiplying it by $2/T$.
On the other hand, by applying the Carr and Madan methodology to the same payoff function, (4.1) via eq. (3.9) with $\kappa = S_0$ we get:

$$f(S_T) = \frac{1}{S_0}\left[\int_0^{S_0} \frac{1}{K}(K - S_T)^+ \, dK + \int_{S_0}^{\infty} \frac{1}{K}(S_T - K)^+ \, dK\right], \tag{4.3}$$

that is a portfolio of continuum of OTM put and call options. From eq. (4.2) and (4.3)

$$\begin{aligned} Gamma =& \frac{2}{TS_0}\left[\int_0^{S_0} \frac{1}{K}(K - S_T)^+ \, dK + \int_{S_0}^{\infty} \frac{1}{K}(S_T - K)^+ \, dK\right] \\ & - \frac{2}{TS_0}\int_0^T \ln\left(\frac{S_t}{S_0}\right) dS_t. \end{aligned} \tag{4.4}$$

Similarly to simple variance swaps (or any other forward contract), the fair strike of a gamma swap is the time-0 expectation of *Gamma* under the risk-neutral measure, i.e. $K_{Gamma} = E_0^*[Gamma]$. Note that, we assumed zero risk-free interest rate, hence $dS_t = S_t\sigma(t, \dots)dW_t^*$. It follows that the risk-neutral expected value of the last part of *Gamma* equals to zero.
Therefore, the time-0 value of the fair strike, with notation $C_0(K)$ (and $P_0(K)$) for a call (and respectively put) option stuck at K, is

$$K_{Gamma} = \frac{2}{TS_0}\left[\int_0^{S_0} \frac{1}{K}P_0(K) \, dK + \int_{S_0}^{\infty} \frac{1}{K}C_0(K) \, dK\right]. \tag{4.5}$$

4.4 Corridor and Conditional Variance Swaps

Corridor variance swaps are such contracts which payoffs depend on the realized variance over only those intervals where the price of the underlying lies in a pre-specified range, i.e. a corridor, C.

The payoff function of such a contract at expiry, T

$$X_{Corr}(T) = (Corr - K_{Corr}) \times N,$$

where K_{Corr} denotes the fair strike, N is the notional and

$$Corr = \begin{cases} \frac{AF}{M} \cdot \sum_{i=1}^{M} \left[\ln\left(\frac{S_i}{S_{i-1}}\right)^2 \cdot \mathbb{1}_{S_{i-1} \in C} \right] & \text{, in discrete-time} \\ \frac{1}{T} \int_0^T \sigma_t^2 \cdot \mathbb{1}_{S_t \in C} \, dt & \text{, in continuous-time.} \end{cases}$$

Depending on the fixing of C, we can distinguish three types of corridor variance swaps. If the corridor is defined as $C = (-\infty, U]$, it is called *Down Corridor Variance Swap*, where U stands for the upper boundary. In the case of $C = [L, \infty)$ we have an *Up Corridor Variance Swap* with L lower boundary. The third case is when the corridor has two finite boundaries: $C = [L, U]$.

Conditional variance swaps are very similar to corridor variance swaps. The difference between the two contracts is the way how the cases when the price is not within the range are treated. The variance is counted as zero outside the corridor in case of corridor variance swaps. At the same time, from the perspective of conditional variance swaps, variance is ignored (i.e. not counted) as long as the price does not lie within the interval. This dissimilarity can be seen from the structure of the payoff function at maturity, T:

$$X_{Cond}(T) = (Cond - K_{Cond}) \times N \times \frac{E}{D},$$

$$Cond = \frac{AF}{M} \cdot \frac{D}{E} \sum_{i=1}^{M} \left[\ln\left(\frac{S_i}{S_{i-1}}\right)^2 \mathbb{1}_{S_{i-1} \in C} \right].$$

Here, D denotes the number of intervals over which the variance is computed through the life of a contract and E is the number of days when the price remains within the required range, that is $E = \sum_{i=1}^{M} \mathbb{1}_{S_{i-1} \in C}$.
Similarly to corridor variance swap, on condition of the type of the corridor we can talk about *Up* ($C = [L, \infty)$) and *Down* ($C = (-\infty, U]$) *Conditional Variance Swaps*.

These derivatives also can be priced by a replicating portfolio without any model specification. This replication strategy is discussed in section 4.4.1.
In [20], Zheng and Kwon manage to determine a pricing formulas for discretely sampled corridor and conditional variance swaps which take the form of one dimensional Fourier integrals. The corresponding continuously sampled fair strike prices are determined as the asymptotic limit of vanishing sampling time interval.
The authors of [18] present a quasi-closed-form pricing formula for the fair strike of a discretely sampled downside corridor variance swap under the 3/2 Stochastic Volatility

Model. Their method is based on the PIDE approach.
An other result for the price of discretely sampled corridor swaps comes from the article [19]. The payoff is decomposed into nested conditional expectations defined across tree nodes by which a stochastic volatility model is approximated.

4.4.1 Model-free replication of Corridor Variance Swaps

Corridor variance swaps also admit model-free replication under the same assumptions as variance and gamma swaps. We wish to find a portfolio which pays the same amount at time T as the corridor variance swap with corridor C, i.e.

$$\frac{1}{T}\int_0^T \sigma_t^2 \cdot \mathbb{1}_{S_t \in C}\ dt.$$

By applying Ito's lemma and the Carr and Madan methodology to the payoff function

$$F(S_T) = \frac{2}{T}\left[\ln\left(\frac{S_T}{S_0}\right) + \frac{S_T}{S_0} - 1\right] \cdot \mathbb{1}_{S_t \in C},$$

it can be shown that the fair strike of a corridor variance swap with corridor $C = [L, U]$ is

$$K_{Corr} = \frac{2}{T}e^{rT}\left[\int_L^{S_0} \frac{1}{K^2}P_0(K)\ dK + \int_{S_0}^{U} \frac{1}{K^2}C_0(K)\ dK\right].$$

This is very similar to the replicating portfolio of a variance swap. The only difference is between the limits of integrals: whereas in the case of a variance swap we need put options with strikes from 0, for a corridor swap put options are needed only with strikes greater than the lower corridor, L. To replicate a corridor swap, call option prices are required with strikes lower than the upper corridor, U. On the contrary, considering a variance swap call options are necessary with strikes until ∞. It follows that the fair strike of a corridor variance swap is lower than the corresponding variance swap's strike.

4.5 Option on realized variance

Options written on realized variance are financial products with payoff at maturity, T considering a call option is:

$$V(T) = \max\left(\sigma_R^2 - K_{var}, 0\right) \times N,$$

where the notations are the same as in section 3. If the value of the corresponding variance swap (at expiration) is positive, the owner of the option receives the difference between the realized variance and the fair variance strike times the notional. Otherwise,

he/she neither receives nor pays anything. This means that he/she can't lose more than the initial option premium. Correspondingly, put options can be written on realized variance, and both call and put options on realized volatility are traded derivatives as well.

4.6 VIX derivatives

The VIX - Volatility IndeX - is an index on Chicago Board Option Exchange, which represents the future expected 30-day US stock market volatility. It's calculated by using real-time, mid option prices written on $S\&P500$ index.

Investors can trade options (since 2006) or future contracts (since 2004) on the VIX index depending on their intentions. By trading these derivatives, similarly to the previously mentioned derivatives on variance - a pure exposure to volatility can be obtained. These products are completely standardized, the details of such trades can be found in CBOE's website, [17].

Chapter 5

Numerical results

This chapter is mainly about the numerical results. Firstly, I present the model calibration method along with its outcomes and check the sensitivity of calibration to different shocks. Then I introduce a method which is used for the simulations. The last part contains the pricing results of various products obtained by different methods. The fair price of a continuously sampled variance swap is determined under the Heston and Bates model. For variance and gamma swaps I applied the pricing method based on their model-independent[1] replicating portfolio and investigated the errors due to the discretization. Moreover, these products, capped, and corridor variance swaps are priced with Monte-Carlo simulation as well. This latter pricing method is suitable for analyzing the impact of jumps which is done in this section in several ways.

For implementation I used *R: The R Project for Statistical Computing*.

5.1 Calibration

In order to get prices close to the observable market prices by a simulation we need to determine the parameters of the selected model. This can be achieved via model calibration. After we have estimated the parameter set, we can price the derivative by simulation or, depending on the model and the type of the derivative by a closed-form expression. The fair variance strike, i.e. the fair price of a variance swap is known under both the Heston and the Bates model. Therefore, my goal was to calibrate these models to the market data through option prices in order to determine the models' parameters by which the variance strikes can be obtained.

[1] but the continuity is an assumption

Although, several methodologies can be found in the literature (e.g. in [16]) for model calibration probably the most popular is to calibrate by minimizing an error function. This function can be defined several ways but it somehow always depends on the difference between the market and the model prices. Assuming that the model and the market prices are denoted by C_i^{Model} and C_i^{Market} respectively, $\forall i = 1, \dots, N$ and N is the number of different quotes, the non-linear optimalization problem can be written as

$$\min \sum_{i=1}^{N} w_i \cdot f(C_i^{Model} - C_i^{Market}). \tag{5.1}$$

An other usual practice to minimize the difference between implied volatilities. In this case, with notations IV_i^{Model} for model and IV_i^{Market} for market implied volatilities, the optimalization formula is the following:

$$\min \sum_{i=1}^{N} w_i \cdot f(IV_i^{Model} - IV_i^{Market}). \tag{5.2}$$

The choice of the weights, w_i-s and $f(\dots)$ is arbitrary in both cases. The most commonly used functions are the square and the absolute value functions.
In my implementation (5.1) was used along with $w_i = 1,\ \forall i$ and $f(\dots) = (\dots)^2$.

From *Bloomberg Terminal* I downloaded the implied volatilities of call and put options on $S\&P500$ index as of 30 November 2017. Details of the market data (spot price of the underlying index, strike prices and maturities of options) is shown in table 5.1. Throughout the implementation the risk-free interest rate and dividend are assumed to be $r = 0$, $d = 0$.

t_0	11/30/2017
T	5/31/2018
S_0	2647.58
$Strike$	2350-2800, by 25[2]
N	25

TABLE 5.1: Market data

In spite of the fact that neither the parameters under the Heston nor under the Bates model are time-dependent, I've calibrated the models only for one maturity. With this simplification a better fit can be generated but just for that slice of the volatility surface, where the time to maturity, $\tau = T - t_0$ corresponds with the life of the options.

[2]The differences between the last 3 strikes are 50.

5.1.1 Parameters of the Heston model

Considering the price and variance dynamics under Heston's model, the parameter set is $\Theta = (v_0, \bar{v}, \kappa, \sigma_v, \rho)$. If we could set these parameters properly, the prices obtained from the semi-closed formula for option prices under the Heston model would be close to the market prices.

The calibration process requires some initial steps. Firstly, we need to determine a primary parameter set, Θ_0 from which the optimalization can start. In conformity with [16], a standard method for defining Θ_0 is to calibrate the model only for a few market data (e.g. 5 option prices). After this initial calibration is done, Θ_0 should be set equals to Θ_0^*, where Θ_0^* stands for the estimated parameter set for the smaller sample.
An other important step to make the parameters remain between specified barriers because of their definition. To get meaningful results we need to be sure about
$v_0,\ \bar{v},\ \kappa,\ \sigma_v > 0$ and $-1 \leq \rho \leq 1$. It can be achieved by defining an *upper* and a *lower boundary* vectors for which $lb \leq \Theta \leq up$. The calibration should be run with this restraint.
Finally, the Feller-condition should be taken into account, though it is not necessary for only mathematical point of view.

Despite a great amount of effort I wasn't able to calibrate the model properly as long as the parameters were forced to satisfy the Feller-condition. The results are shown in figure 5.1.

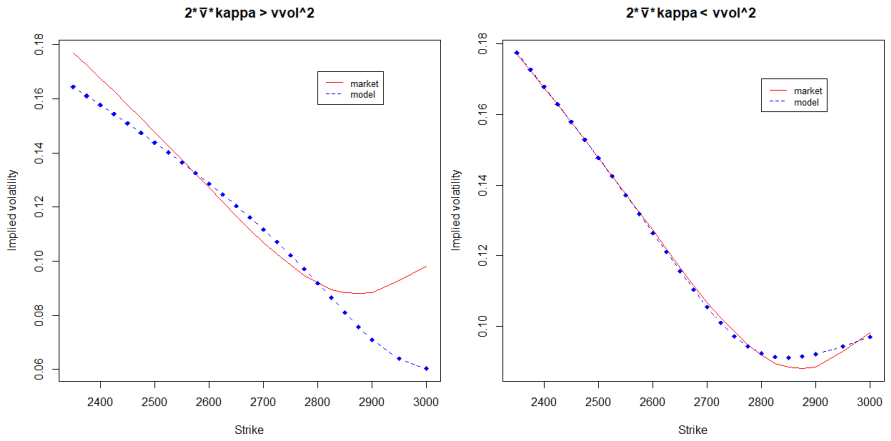

FIGURE 5.1: Fits of the model implied volatilites to market data with parameters fulfilling (left) and violating (right) the Feller-condition.

As we can see, when the calibrated parameters accomplish the Feller-condition, denoted by Θ^1 (on left figure) the shape of the model implied smile greatly differs from the market implied volatility curve. Neither the slope nor the convexity are identical for

the two curves. Therefore, it is considered a weak result. In the second case, when the Feller-condition does not hold true for the estimated parameters the fit is much better. Although, using parameter set 2, Θ^2 means that the variance process can reach zero with positive probability it can be handled with different methods. A few example will be mentioned in the following sections.

parameter set	v_0	$\bar{v}$	κ	σ_v	ρ
Θ^1	0.001206	0.368491	0.185365	0.369609	-0.952493
Θ^2	0.007917	0.148276	0.417199	0.669289	-0.749691

TABLE 5.2: Calibrated parameters of Heston model for which the Feller-condition is true (Θ^1), and not (Θ^2).

I checked how significant is the difference between the estimated parameters if the market data is shocked somehow. The various shock types are denoted by letters from A to K. Firstly, all market observed implied volatility were shifted parallel by a constant, 0.01 down (by subtraction) and up (by addition) marked by cases A and B, respectively. In cases C, D, E, F, G and H all market data were shocked by a different multiplicative factor. These multipliers are 90%, 95%, 99%, 101%, 105% and 110%, correspondingly. Finally, in the last three examples only one market data, that belongs to strike $K = 2775$ was shocked differently. I denotes the case when the shift was small, the new value remained between the real value of its neighbours. This can be thought of as a price change due to market movements. In the case of J the shock is grater. K stands for a huge change as it was a wrong data point. In table 5.3 below, the relative changes (in the parameters) are shown compared to the initial model parameters (which were obtained by model calibration to the original dataset).

	Δv_0	$\Delta\bar{v}$	$\Delta\kappa$	$\Delta\sigma_v$	$\Delta\rho$
A	-0.25	-0.04	-0.10	-0.08	0.02
B	0.89	-0.06	-0.21	-0.12	0.00
C	-0.42	-0.09	-0.12	-0.25	0.01
D	-0.36	-0.02	0.00	-0.09	0.00
E	-0.06	0.00	0.00	-0.01	0.00
F	-0.18	0.16	-0.06	0.00	0.03
G	-0.03	0.21	-0.01	0.07	0.04
H	0.67	0.08	0.01	0.13	0.04
I	-0.03	-0.02	0.00	-0.06	0.02
J	-0.03	0.00	-0.01	-0.07	0.03
K	-0.01	0.02	-0.01	-0.01	0.00

TABLE 5.3: Impact of the shocked market to the model parameters.

Some observations can be made from this comparative table. For example, we can notice greater - absolute - values in Δv_0 but it is possibly a consequence of the division by the initially small v_0. An other note: the correlation parameter, ρ seems to be the most

stable. In the last three cases, when only one point is shocked, the parameters don't alter too much, even in case K.

Figure 5.2 shows the shocked market data and the corresponding model implied volatilities[3]. In all plots, the solid lines represent the (shocked) market observed volatilities and the broken lines with dots illustrate the model implied volatilities. On the left graph the

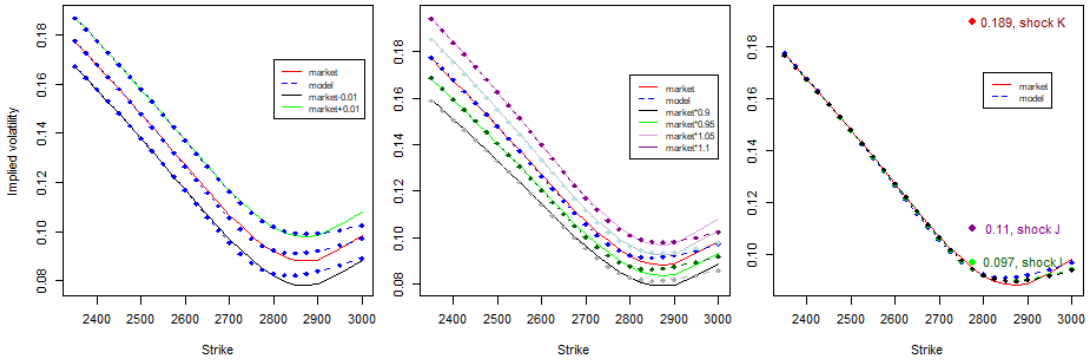

FIGURE 5.2: Calibration results to shocked market data under Heston's model

first two cases, A, B and the original example are shown. On the second picture, C, D, G and H states[4] are plotted along with the original one. On the right figure, the last three and the initial cases are shown. As it can be seen, the results from the different calibrations are very similar in spite of the shocked points. From these results, we can conclude that the model calibration is fairly stable.

An other test was performed to analyze the effects of parameter modifications. First of all, miscellaneous percentiles, (90%, 95%, 99%, 101%, 105% and 110%) of the estimated parameters were computed separately. Using these modified parameters - it is important that just one is changed at a time - the option prices and the implied volatilities were calculated under the Heston model. Figure 5.3 shows the error between the market data and the model implied volatilities supposing one parameter has been changed. The solid, red line is used for plotting the original[5] error.

The correlation parameter of Heston model, ρ (rho on the graphs) affects the rise of the implied volatility curve. The simile is symmetric when $\rho = 0$, downward sloping when $\rho < 0$ and upward sloping if $\rho > 0$. In all cases, the shifted parameter was negative. From the graph we can see that if we increase (decrease) the value of κ, the slope becomes more negative (positive) therefore, the discrepancies increase on the wings.

The effects of shifts on parameters $V0$ and vm (these two represent the initial variance, v_0 and the long-run variance, $\bar{v}$, respectively) are very similar. The different errors are

[3]The model implied volatilities are obtained from the parameters of the calibrated models. Here, the calibrations were intended to match the shocked market data.

[4]E and F are left out from the illustration since the values in those cases are too close to the original one and the appearance would be ruined.

[5]model implied volatilities along with parameter set Θ_2 minus market implied volatilities

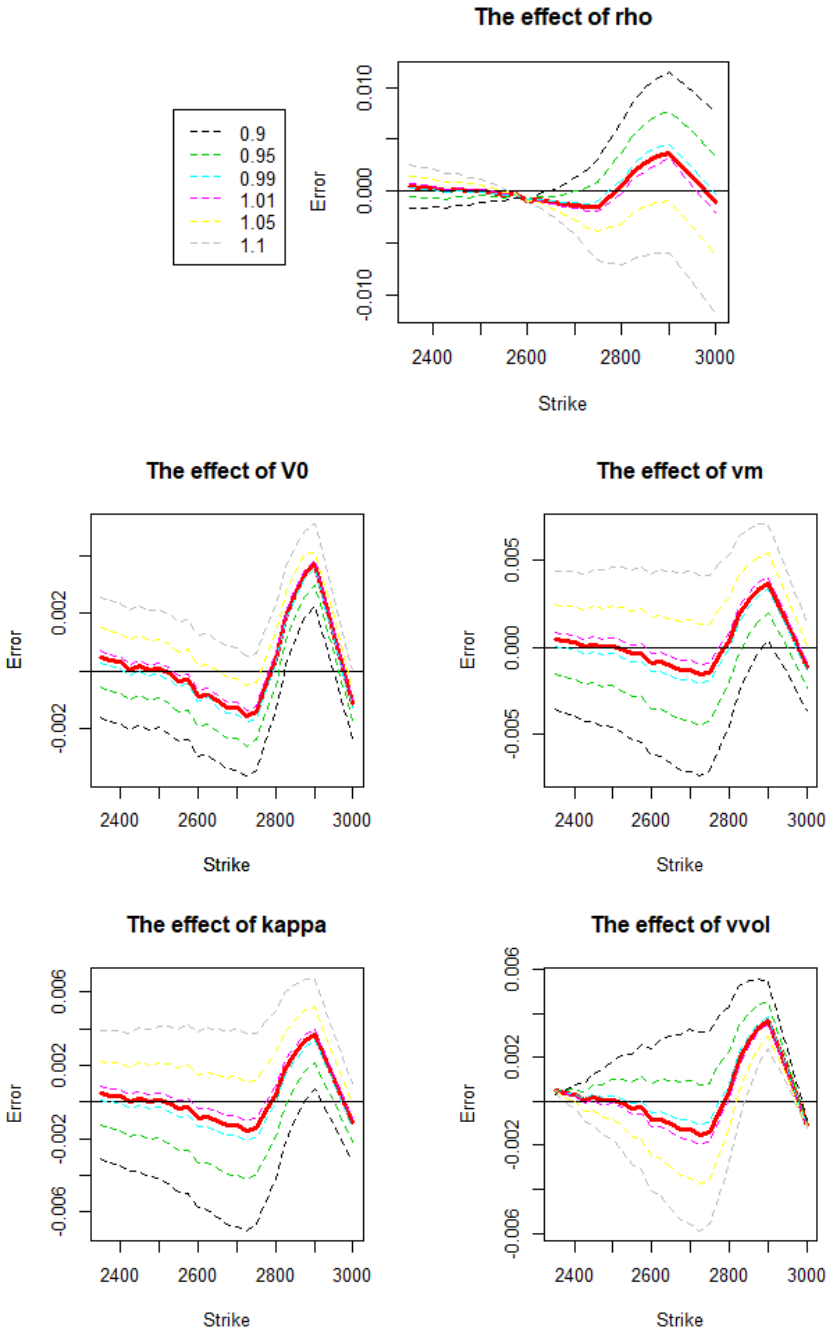

FIGURE 5.3: Effects of parameter changes under the Heston model

parallel to one another in both cases. It can also be concluded that the further the value of the shifted parameter from the original one is, the higher (in absolute value) the discrepancies are. From these results we can observe that these parameters affect the level of the implied volatility smile.

Almost parallel shifts can be noticed in the case of parameter *kappa* which denotes the speed of mean-reversion, κ. The errors are the largest where the strike price is close to the initial price. On the wings, where the strikes are far from the spot price, the

discrepancies are smaller. This is in line with the role of κ, it controls the depth of the smile.
Parameter σ_v (represented by *vvol*) also affects the depth of the smile but inversely compared to κ. As σ_v increases, the smile becomes more characteristic. On the other hand, as κ increases, the smile becomes flat. These two parameters usually control each other.

5.1.2 Parameter estimation under the Bates model

Similarly to the calibration process under the Heston model, the parameter set can be estimated under the Bates model as well. The model implied prices can be determined by applying the semi-closed formula for option prices supposing the dynamic of the underlying price process follows eq. 2.7. Now we have eight parameters to which we need to calibrate the model: $\Theta = (v_0, \bar{v}, \kappa, \sigma_v, \rho, \lambda, \mu_J, v_J)$.

The steps are the same as under Heston's model. After determining an initial parameter set, Θ_0 we can run the calibration process along with the constraints for the parameters. Also, the Feller-condition should be kept in mind.

Notwithstanding that the calibration wasn't successful under the Heston model as long as the Feller-condition was considered, in this case a satisfactory result can be obtained. This favourable outcome can be the result of the model's greater degree of freedom[6] compared to the Heston model. However, the calibration was also run without the Feller condition to compare the resulting fits and the parameters. The estimated parameters and the realized fits are shown in table 5.4 and figure 5.4, respectively.

parameter set	v_0	$\bar{v}$	κ	σ_v	ρ
Θ^1	0.000316	0.026969	2.122509	0.338356	-0.82
Θ^2	0.009698	0.015926	4.470985	0.594736	-0.826437

λ	μ_J	v_J
0.097033	-0.21733	0.080799
0.1015	-0.121055	0.065577

TABLE 5.4: Calibrated parameters of the Bates model for which the Feller-condition is true (Θ^1), and not (Θ^2).

[6] A greater degree of freedom is not undoubtedly beneficial, it can cause complications as well.

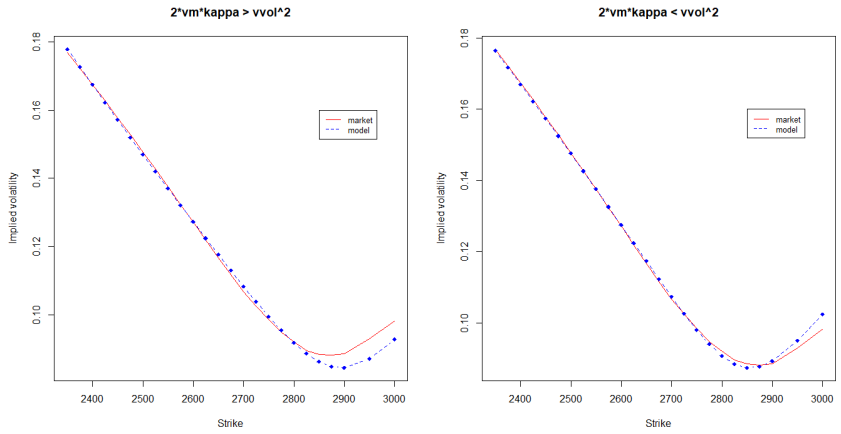

FIGURE 5.4: Market and model implied volatilites under the Bates model along with parameters shown in table 5.4.

Just like in the case of Heston's model, a test was run in order to inspect the effects of parameter variations. Here, parameter set Θ^1, which satisfies the Feller-condition is considered as the default choice. These values are shifted individually by various multiplicative factors : 90%, 95%, 99%, 101%, 105% and 110%. The results are shown in figure 5.5 and 5.6.

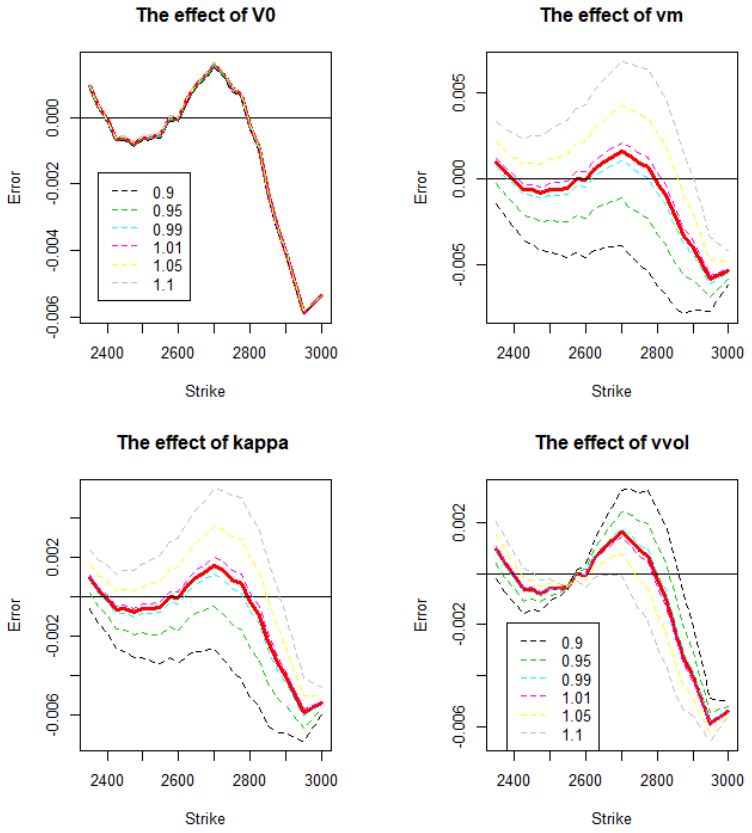

FIGURE 5.5: Errors of model and market implied volatilities due to the change in the first four parameters of Bates model.

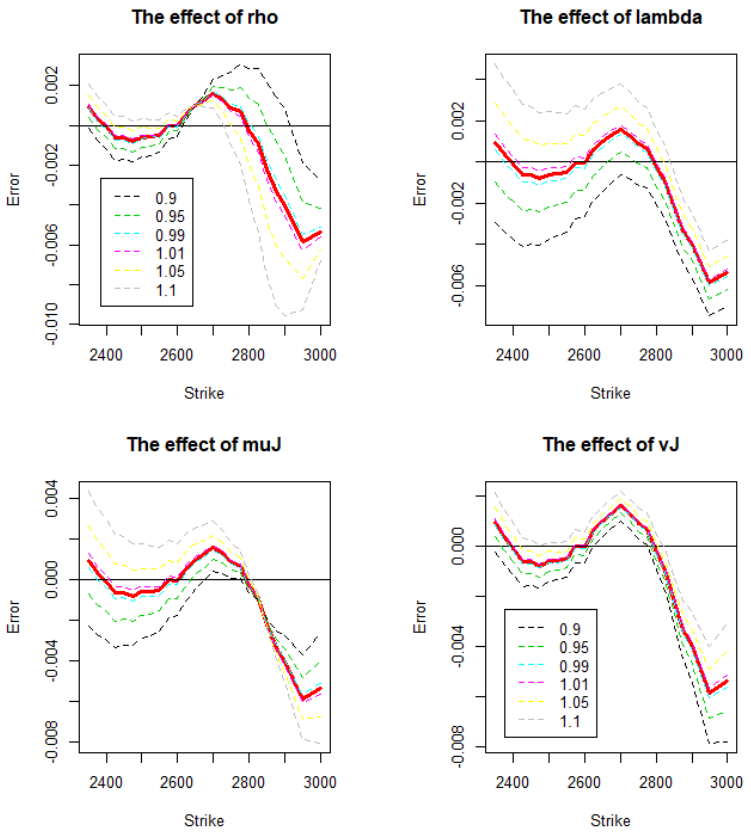

FIGURE 5.6: Errors of model and market implied volatilities due to the change in the last four parameters of Bates model.

Considering the effects of parameters which are in the Heston model as well (v_0, $\bar{v}$, κ, σ_v and ρ) the same conclusions can be made.

Parameter μ_J similarly affects the smile as ρ does. Its effect is mainly appears in the slope of the smile. For negative (positive) values the curve is downward (upward) sloping. If we increase μ_J (in this case, since the calibrated value is negative, this means that μ_J becomes more negative), the slope of the implied volatility curve becomes more negative and the errors on the wings increase in absolute value.

On the other hand, the two remaining jump parameters, both v_J and λ affect the kurtosis[7] of the distribution of the asset's returns. Higher values of v_J lead to a higher variance in the size of jumps in the asset's price process. Correspondingly, the higher the value of λ is, the more jumps happen in the price, therefore the overall volatility increases.

Unfortunately, I could not calibrate the Bates model to shocked market data, therefore I didn't execute the other test performed in the previous section for Heston model.

[7]These features can not really be seen on the graphs.

5.2 Simulation

Since the mathematical derivations of different models are generally considered in the continuous time horizon (for instance, in our case the Heston and the Bates models) we need to discretize the processes under these models in order to simulate the market. Here, I'm going to show briefly a few techniques, covered by [16] to simulate the discretized processes.

Apparently, the most standard and straightforward method to discretize a continuous process is the *Euler Scheme*, which is a first-order approximation.
Suppose that the dynamic of a process, X_t is given in the form of

$$dX_t = \mu(X_t, t)dt + \sigma(X_t, t)dW_t. \tag{5.3}$$

By integrating both sides of this equation from t to $t + \Delta_t$, we obtain the value of $X_{t+\Delta_t}$ such as,

$$X_{t+\Delta_t} = X_t + \int_t^{t+\Delta_t} \mu(X_u, u)du + \int_t^{t+\Delta_t} \sigma(X_u, u)dW_u.$$

Applying the Euler Scheme means that we approximate the integrals by the left Riemann sum:

$$\int_t^{t+\Delta_t} f(x)\ dx \approx \sum_{i=t}^{t+\Delta_t} f(x_i)\Delta x_i = f(t)\Delta_t.$$

Note that, the left point rule need to be used because we do not have information about the future value of $\mu(X_s, s)$ and $\sigma(X_s, s)$ at time t, where $t < s$, which would be essential for estimating the integrals by for instance the right Riemann sum. Thus, the discretized formula is

$$\begin{aligned} X_{t+\Delta_t} &= X_t + \mu(X_t, t)\Delta_t + \sigma(X_t, t)\left[W(t + \Delta_t) - W(t)\right] \\ &= X_t + \mu(X_t, t)\Delta_t + \sigma(X_t, t)\sqrt{\Delta_t}Z, \end{aligned}$$

where $Z \sim N(0, 1)$, and the well-known property of the Brownian motion's increment, $W(t + \Delta_t) - W(t) \overset{d}{=} \sqrt{\Delta_t}Z$ was considered.

Although, the underlying price and variance dynamics under the Heston model (2.3, 2.4) can be written in the form of eq. (5.3), the Euler discretization method is not suitable for the simulation by itself. The main reason is that the value of the variance process, v_t can turn into negative even if the parameters fulfill the Feller-condition. This is a result of the discretization, since the proposition about the non-negativity in accordance with the Feller-condition is only valid under continuous time. In my implementation, under the Heston model the calibration was not successful as long as the Feller-condition was

considered, therefore generating negative values in the variance process is more likely. This should be handled appropriately.

One way to avoid negative values in the variance process using the Euler Scheme is to replace the value of the variance at time t, v_t by $max(0, v_t)$, everywhere in the discretization formula. This method is called *full truncation scheme*. A disadvantage of this approach that zero variances are produced, however, that is not typical for price processes on the market.
An other solution for preventing negative values under the Euler discretization can be the application of the *reflection scheme*. In this case the absolute value of the variance, $|v_t|$ should be put in the place of v_t, everywhere in the discretization formula where v_t would appear.
Both of these methods are fairly biased but on the other hand, implementing these techniques is very simple.

The variety of analogous methods is pretty board. On the basis of the comparison of different simulation methods in [16], I have chosen a procedure regarding the biases caused by the methods, the difficulty of the implementations and time-efficiency. In the next section the selected method, namely the *Quadratic Exponential Scheme* proposed by Andersen will be presented by following his original article, [1].

5.2.1 QE Scheme

As it was pointed out in section 2.3.1, $v_{t+\Delta_t}$ follows non-central chi-squared distribution on condition of the value of v_t with $\lambda = 2c_t v_t e^{-\kappa\Delta_t}$ non-centrality parameter. The main idea of this method is to sample from an approximation of the non-central chi-squared distribution depending on the size of λ which is equivalent to sampling in respect of the volume of v_t.
In the case of a smaller value of v_t, the approximated density for the non-central chi-squared distribution can be expressed as

$$Pr(v_{t+\Delta_t} \in [x, x+dx] \approx \left(p\delta(0) + (1-p)\beta e^{-\beta x}\right) dx, \tag{5.4}$$

where δ denotes the Dirac-delta function, $p \in [0, 1]$ and the exact value of p and β is fixed to match the first two moments of the variance process. The inverse distribution function can be obtained by integrating the previous equation and inverting it:

$$\Psi^{-1}(u) = \begin{cases} 0 & , \text{ for } p \leq u \leq 1 \\ \frac{1}{\beta} \ln \frac{1-p}{1-u} & , \text{ for } p \leq u \leq 1. \end{cases}$$

Thus, the value of $v_{t+\Delta_t}$, if v_t is small and U_V denotes a uniform random number, is

$$v_{t+\Delta_t} = \Psi^{-1}(U_V). \tag{5.5}$$

For higher values of v_t, the approximation method is different. Supposing $Z_V \sim N(0,1)$, a random variable with non-central chi-squared distribution can be approximated by

$$v_{t+\Delta_t} = a(b + Z_V)^2, \tag{5.6}$$

where a and b are constants, and determined by moment-matching. Now, the Quadratic Exponential Scheme is defined by eq. (5.5) and (5.6).

In order to choose the parameters, $a,\ b$ and $p,\ \beta$ correctly we need to take the conditional expectation, eq. (2.5) and variance, eq. (2.4) into account. Lets denote these values by m and s^2, respectively.

$$\begin{aligned} m =& E\left[v_{t+\Delta_t}|v_t\right] = (v_t - \bar{v})e^{-\kappa\Delta_t} + \bar{v} \\ s^2 =& D^2\left[v_{t+\Delta_t}|v_t\right] = \frac{\sigma_v^2}{\kappa} v_t \left(e^{-\kappa\Delta_t} - e^{-2\kappa\Delta_t}\right) + \frac{\bar{v}\sigma_v^2}{2\kappa}\left(1 - e^{-\kappa\Delta_t}\right)^2 \end{aligned}$$

Firstly, lets concentrate on the case when v_t is large, and find a and b. It is well-known that if $Z_V \sim N(0,1)$ than $Z_V^2 \sim \chi_1^2$, where 1 denotes the degree of freedom. It follows that $E(v_{t+\Delta_t}) = a(1+b^2)$ and $D^2(v_{t+\Delta_t}) = 2a^2(1+2b^2)$. These should be made equal to m and s^2, respectively. After rearranging the equations the expressions for a and b are the following:

$$\begin{aligned} b^2 &= \frac{2}{\Psi} - 1 + \sqrt{\frac{2}{\Psi}\left(\frac{2}{\Psi} - 1\right)}, \\ a &= \frac{m}{1+b^2}, \end{aligned}$$

where $\Psi = s^2/m^2$, and $\Psi \leq 2$ is obligatory for the existence of b.
On the other hand, when the volume of v_t is small, the expectation and the variance are different. In this case we can derive the formulas by applying the mathematical definition of the first two moments. By integrating the density function, eq. (5.4) directly, we get $E(v_{t+\Delta_t}) = (1-p)/\beta$ and $D^2(v_{t+\Delta_t}) = (1-p^2)/\beta^2$. Again, for defining p and β the conditional expectation and variance need to be matched with m and s^2, respectively. Defining Ψ as previously, the solution is

$$p = \frac{\Psi - 1}{\Psi + 1}, \quad \beta = \frac{1-p}{m}.$$

So that $0 \leq p \leq 1$ holds, Ψ has to be greater than, or equal to 1.

For now, we have two different sampling method on condition of the magnitude of v_t but do not have any rule for selecting the proper scheme. As Andersen mentions in his work, one of the following disparities will always be true: $1 \leq \Psi$, or $\Psi \leq 2$. Therefore we can use one of the sampling schemes for sure. Introducing a new constant, $\Psi_c \in [1, 2]$ the decision regarding the model choice can be made. Andersen suggests to set $\Psi_c = 1.5$, so that, if $\Psi \leq \Psi_c$ (5.6) method should be used and (5.5) otherwise. Table 5.5 summarizes the required steps under the QE Scheme.

1. Given v_t, compute m, s^2 and Ψ.
2. Fix a value from distribution $U_V \sim U(0, 1)$.
3. If $\Psi \leq \Psi_c$: compute a, b, and $Z_V := \Phi^{-1}(U_V)$. Then $v_{t+\Delta_t} := a(b + Z_V)^2$.
4. If $\Psi > \Psi_c$: determine p, β. Then $v_{t+\Delta_t} := \Psi^{-1}(U_V)$, where $\Psi^{-1}(u)$ defined by eq. (5.5)

TABLE 5.5: Steps of the Quadratic Exponential Scheme

The main advantage of applying this method for simulating the variance process is that it will not produce negative values for v_t. Also, the implementation is traceable and the computational time is reasonable as well.

5.2.2 Simulation of the underlying price process

In theory, similarly to the case of the variance process the Euler scheme can generate negative values for the underlying price process as a consequence of the discretization. Though it is not as feasible as in case of the variance, simulating the log price process and then exponentiating it is a standard method for avoiding this drawback.
We can obtain the log price dynamic by applying Ito's lemma to eq. (2.3). The log price process under the risk-neutral measure, provided that $r = 0$ is the following

$$d \ln S_t = -\frac{1}{2}\, v_t\, dt + \sqrt{v_t}\, dW_t^S$$

and it is in integral form, considering the Cholesky decomposition, $dW_u^S = \rho\, dW_u^v + \sqrt{1-\rho^2} dW_u$, where dW_u is independent of dW_u^v :

$$\ln S_{t+\Delta_t} = \ln S_t - \frac{1}{2}\int_t^{t+\Delta_t} v_u\, du + \int_t^{t+\Delta_t} \sqrt{v_u}\, \rho\, dW_u^v + \int_t^{t+\Delta_t} \sqrt{v_u}\sqrt{1-\rho^2}\, dW_u. \quad (5.7)$$

Andersen also suggests a method for simulating the log-price process in [1] which should be used along with the QE Scheme. He explains that using the Euler method to discretize

the dynamic of the log price can easily lead to weak results due to the wrongly fixed correlation among the Brownian motions.
From the integral form of v_t,

$$v_{t+\Delta_t} = v_t + \int_t^{t+\Delta_t} \kappa\ (\bar{v} - v_u)\ du + \sigma_v \int_t^{t+\Delta_t} \sqrt{v_u}\ dW_u^v$$

we can express the last but one part of eq. (5.7), that is

$$\int_t^{t+\Delta_t} \sqrt{v_u}\ dW_u^v = \frac{1}{\sigma_v}\left(v_{t+\Delta_t} - v_t - \int_t^{t+\Delta_t} \kappa\ (\bar{v} - v_u)\ du\right).$$

Substituting this to eq. (5.7), we get

$$\begin{aligned}\ln S_{t+\Delta_t} = \ln S_t + \frac{\rho}{\sigma_v}\left(v_{t+\Delta_t} - v_t - \kappa\ \bar{v}\ \Delta_t\right) + \left(\frac{\kappa\rho}{\sigma_v} - \frac{\rho}{2}\right)\int_t^{t+\Delta_t} v_u\ du \\ + \sqrt{1-\rho^2}\int_t^{t+\Delta_t} \sqrt{v_u}\ dW_u. \end{aligned} \tag{5.8}$$

In order to discretize the log price process, the time-integral of v_t should be handled somehow. One suggestion for that is to approximate it with the Euler Scheme, i.e.

$$\int_t^{t+\Delta_t} v_u\ du \approx v_t \Delta_t.$$

The distribution of the integral in the last part in eq. (5.8) is known, since dW_u is independent of dW_u^v. It follows normal distribution with zero expectation and $\int_t^{t+\Delta_t} v_u\ du$ variance. Applying the previously proposed approximation for the time-integral of v_t,

$$\int_t^{t+\Delta_t} \sqrt{v_u}\ dW_u \overset{d}{=} \sqrt{v_t \Delta_t} \cdot Z,$$

where Z is a standard normal variable.
Summarizing the previous steps and introducing some new constants,

$$K_0 = -\frac{\rho}{\sigma_v}\kappa\ \bar{v}\ \Delta_t, \quad K_1 = \left(\frac{\kappa\rho}{\sigma_v} - \frac{\rho}{2}\right)\Delta_t - \frac{\rho}{\sigma_v}, \quad K_2 = \frac{\rho}{\sigma_v}, \quad K_3 = \left(1-\rho^2\right)\Delta_t,$$

the discretization formula of the log price process:

$$\ln S_{t+\Delta_t} = \ln S_t + K_0 + K_1 \cdot v_t + K_2 \cdot v_{t+\Delta_t} + \sqrt{K_3\ v_t} \cdot Z,$$

where $Z \sim N(0,1)$. The dynamic of the price of the underlying can be easily expressed from the log price process, such as

$$S_{t+\Delta_t} = S_t e^{K_0 + K_1 \cdot v_t + K_2 \cdot v_{t+\Delta_t} + \sqrt{K_3\ v_t} \cdot Z}.$$

This equation is adequate for the simulation of the Heston model's dynamic.

However, this method doesn't cover the simulation of jumps. Under the Bates model, the independence of the Poisson-process (N_t) and the relative jump size (Y_i) of (one other and) the Brownian motions (W^S and W^v) is an assumption. It follows that we can simulate the jump-part independently and than add it to the log price process.

5.3 Pricing

Generally, several potential pricing method can be used for valuing a derivative. In this thesis I collected some well-known pricing models of variance swaps: the value of these derivatives can be obtained by their model-independent replicating portfolio. Also, its fair strike can be determined under the Heston and the Bates model and we can price them via Monte-Carlo Simulation as well. For gamma and corridor variance swaps, the model-free pricing method is also available. Moreover, Monte-Carlo Simulation can be used for calculating the price of e.g. gamma swaps, corridor swaps, capped variance swaps or any other derivatives (also the listed ones in section 4).
I implemented these means in order to get prices and compare them. During the whole implementation the following assumptions hold, unless otherwise stated: the risk-free interest rate is zero and the underlying ($S\&P500$ index) does not pay dividends. The spot price is $S_0 = 2647.58$ as it was observed as of 11/30/2017. The number of simulated paths in the Monte Carlo simulation is 10000 and the difference between two consecutive observation day is 1/365, i.e. daily sampled variance was calculated. The annualization factor, AF is assumed to be 365. In order to get prices under the Heston model, I used the calibrated parameter set which violates the Feller-condition, Θ^2 from table 5.2. On the contrary, concerning the Bates model, parameter set Θ^1 is used from table 5.4 which satisfies the Feller-condition.

5.3.1 Model-free pricing and the effect of discretization

I approximated the fair price of a variance swap and a gamma swap by determining the values of their replicating portfolio. These portfolios consist of vanilla call and put options as it was mentioned before. The fair strikes are given in the continuous world by equations (3.11) and (4.5). In the discrete time horizon, this value can be approximated by replacing the integrals with sums and dK-s with ΔK-s.
Although option prices are not available for all strikes, we can estimate them even with strikes out of the initial strike range. This process can be done by using the SVI parametrization of implied volatility, proposed by Gatheral in [11]. In this methodology,

the implied volatilities are modelled by the following equation:

$$v(x) = \sigma_{BS}^2(x) = a + b\left(\rho(x-m) + \sqrt{(x-m)^2 + \sigma^2}\right),$$

where $x = \ln(K/F_T)$, K is the strike, F_T is the future price of the underlying at maturity, T and $a,\ b,\ \rho,\ m,\ \sigma$ are the model's parameters. After determining the parameters by calibration to market data, one can estimate implied volatilities of options with any arbitrary strikes. Finally, the option prices are given by the Black-Scholes formula.
On figure 5.7 the observed and estimated implied volatilites are plotted when $\Delta K = 25$ and the strike range is $[2200, 3100]$. For those strikes for which option prices weren't available, an estimated value was calculated by the SVI parametrization.

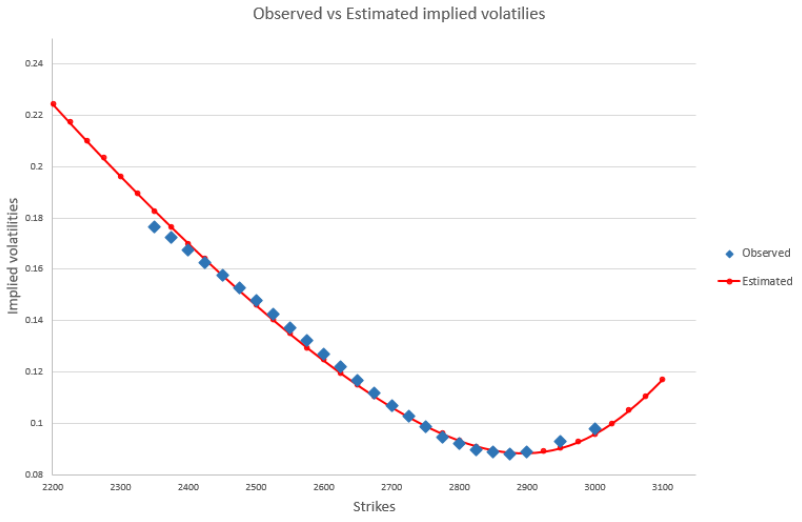

FIGURE 5.7: Observed and Estimated Implied Volatilities by SVI parametrization. The strike range is $[2200, 3100]$ and the difference between two strikes, $\Delta K = 25$.

I studied the variation of variance and gamma swaps' prices in two ways: I increased the strike range and decreased the difference between strikes. The examined strike ranges are the initial one $[2350, 3000]$ and three wider intervals: $[2200, 3100]$, $[2000, 3300]$ and $[1900, 3400]$. In all cases, the value of a gamma and a variance swap were calculated while the difference between strikes is 25 (as originally), 10, 5 and 1. The results are shown in figure 5.8 below. On this plot the values of the variance swaps are marked with blue color and the red symbols stand for gamma swaps, respectively. This outcome shows similar attributes as in section 3.1.1, where I examined the impact of various violations of the assumptions made under the model-independent replication. Here - using real market data - the following comments are right: for a given strike range (denoted by a fixed type of symbol, e.g. a square), the fair strike of a variance (and gamma) swap decreases as the step size between the strikes (ΔK) decreases. We can observe greater differences between the values of variance and gamma swaps for wider intervals. Moreover, if we

fix the step size and increase the breadth of the strike range, the value of the variance (and the gamma) swap increases. Since the model-free replication assumes there isn't any jump in the underlying price process, I compared these values to the continuous fair variance strike under the Heston model which (also assumes continuity, and) is illustrated by a blue, dashed line. Ideally, we should see that as $\Delta K \to 0$ and (in case of $K \in [L, U]$)

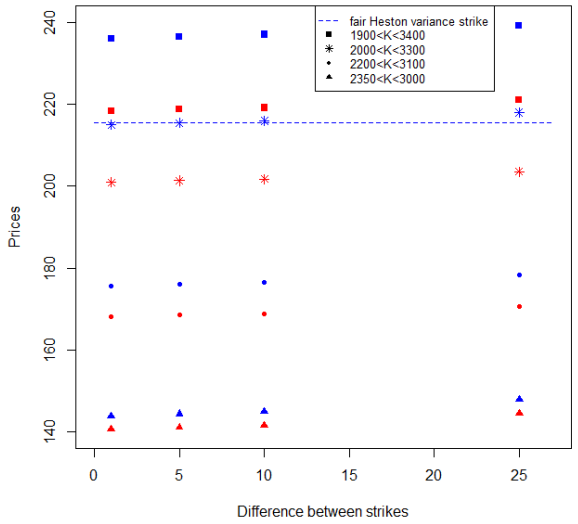

FIGURE 5.8: The values of the replicating portfolios of variance and gamma swaps for different strike ranges and for different step sizes between the strikes. Blue symbols mark the fair variance strikes and the red ones denote the different gamma swap's prices.

$L \to 0,\ U \to \infty$, the fair variance strike $K_{var}^{rep} \to K_{var}^{Hest}$. However, this value is exceeded in this implementation when the strike range is $[1900, 3400]$. Probably, this deviation is caused by the errors which were made by the calibrations[8]. For example, we can notice on figure 5.7 that the estimated volatilities might be higher for smaller strikes (for put options) than the original smile would imply.

5.3.2 Pricing under the Heston and the Bates model

All results shown in this section are obtained under a specified dynamics and therefore depend on the models' parameters.

[8]Two calibration were made: one for the Heston model (and therefore for the fair variance strike) and an other for the SVI parametrization.

5.3.2.1 Variance and Gamma Swaps

Firstly, I computed the value of a variance swap under the Heston model. The continuously sampled fair variance strike is given by eq. (3.12). With the corresponding parameters, the resulting fair strike is $K_{var} = (14.68)^2$, expressed in squared-percentage. For comparison, the following table shows the different fair variance strikes, obtained by Monte-Carlo Simulations - assuming the market follows the Heston's dynamics with the calibrated parameters (Θ^2). In the second row, the fair strikes of a gamma swap are shown for seven different Monte-Carlo run but with the same parameters. The simulated

MC run	1st	2nd	3rd	4th	5th	6th	7th
K^H_{var}	$(14.67)^2$	$(14.70)^2$	$(14.65)^2$	$(14.46)^2$	$(14.56)^2$	$(14.71)^2$	$(14.86)^2$
K^H_{gamma}	$(14.09)^2$	$(14.14)^2$	$(14.08)^2$	$(13.94)^2$	$(14.28)^2$	$(14.53)^2$	$(13.85)^2$

prices of variance swaps are scattered around the fair variance strike determined under the Heston model. In all cases, the price of the corresponding gamma swaps are lower than the variance strikes as expected.

Similarly, the fair variance strike of a variance swap can be easily obtained under the Bates model by eg. (3.13). In this case the continuously sampled fair strike is $K_{var} = (12.54)^2$. The corresponding Monte-Carlo variance prices and fair strikes of a gamma swap (attained via MC simulation as well) under the Bates model are the following:

MC run	1st	2nd	3rd	4th	5th	6th	7th
K^B_{var}	$(12.61)^2$	$(12.24)^2$	$(12.48)^2$	$(12.37)^2$	$(12.45)^2$	$(12.36)^2$	$(12.44)^2$
K^B_{gamma}	$(11.92)^2$	$(11.63)^2$	$(11.81)^2$	$(11.73)^2$	$(11.79)^2$	$(11.72)^2$	$(11.78)^2$

Analogous conclusion can be made under the Bates model. The simulated variance strikes not vary excessively from the fair price of the variance swap and the simulated gamma strikes are lower than the corresponding variance strikes in all cases.
As we can see - by using the corresponding calibrated parameters - under the Heston model, the strikes of variance and gamma swaps are greater than in the Bates model. Additionally, from these data we can deduce to the stability of Monte-Carlo Simulation on 10000 paths, since the simulated prices are close to their theoretical values.

Next, I examined how the prices of variance and gamma swaps are affected by the different jump parameters. I used the Bates dynamics along with the calibrated Heston parameters. From the three jump parameters, in each cases two were assumed to be fixed numbers. The prices are plotted as a function of the third jump parameter and are expressed in squared-percentage[9]. Figure 5.9 below shows the prices of variance and gamma swaps as a function of the jump intensity, λ. The expected value of the relative

[9]For example, the fair variance strike under the Heston model is $K_{var} = (14.68\%)^2 \approx 215.5$.

jump size, μ_J is fixed at 0 and the standard deviation of the relative jump size, v_J is 0.1.

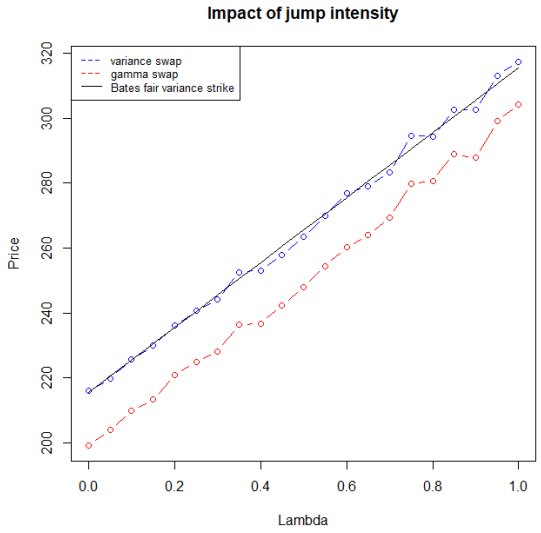

FIGURE 5.9: Prices of variance and gamma swaps as a function of λ. $\mu_J = 0$ and $v_J = 0.1$.

By increasing the value of the jump intensity, the number of jumps increases and therefore greater realized variance is expected. Exactly this can be seen on figure 5.9. An other remark which is also verified by the formula of the fair variance strike under the Bates model (eq. 3.13), is the linear dependence of the variance swap's price on λ. We can see that with these parameters, for all λ, the price of the variance swap is greater than the gamma swap's. It is always the case as long as the distribution of the underlying's return is skewed to the left[10].

On the next figure 5.10, the prices of variance and gamma swaps are plotted as a function of the expected value of the relative jump size, μ_J. The jump intensity, λ is fixed at the calibrated value under the Bates model ($\lambda = 0.09703$) and the standard deviation of the relative jump size, v_J is assumed to be 0, i.e. if a jump happens, the size of the jump is constant.

As long as the expected value of the jump size is negative (the skew is downward sloping), the value of the variance swap is greater than the gamma swap's. When μ_J reaches zero the gradient of the gamma swap's value becomes steeper than the variance swap's. This means that after a while - when the effect of the expected positive jump size is large enough - the fair strike of the gamma swap will be higher. In this example, the turning point is at approximately $\mu_J = 0.24$. An other property we can notice is the symmetry of the variance swap's price. Since the continuous fair variance strike under the Bates model depends on the squared expected jump size, the sign of μ_J doesn't matter, just

[10]Downward sloping skew is a stylized fact on financial markets.

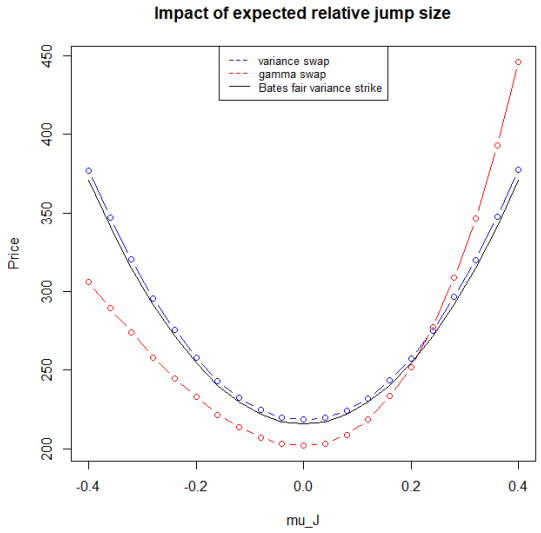

FIGURE 5.10: Fair variance strikes of gamma and variance swaps for different expectations of relative jump sizes. $\lambda = 0.09703$ and $v_J = 0$.

its distance from 0. On the contrary, the gamma swap's price is not symmetric. On this graph, an other feature of gamma swaps is observable: when negative jumps are expected, the gamma swap underestimates the realized variance. This means that gamma swaps are less sensitive to large downside movements in the underlying's price than variance swaps. Considering positive expected jumps, the gamma swap overestimates the realized variance, so that a greater gamma strike is expected to be fair than the variance swap's strike.

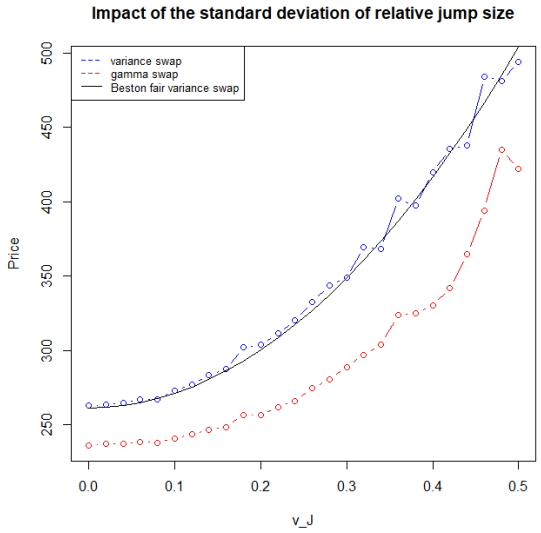

FIGURE 5.11: Fair variance strikes of gamma and variance swaps for different volatilities of relative jump sizes. $\lambda = 0.09703$ and $\mu_J = -0.21733$

Figure 5.11 shows the realized prices of variance and gamma swaps as the jump's volatility

increases. The other two jump parameters, λ and μ_J correspond with their calibrated value under the Bates model. On this figure we can also see the squared dependence of the variance strike on v_J as it is expected by the formula of the fair variance strike under the Bates model (eq. 3.13). Moreover, it is also reasonable that as the standard deviation of jump sizes increases, the simulated variance strikes more likely differ from its fair value. Although these are results of a simulation and therefore the values are different for all MC run (not fixed), for small values of v_J the simulated variance strikes are very close to the fair Bates strike. On the other hand, for larger v_J-s the simulated prices vary more on average from the fair variance strike.

5.3.2.2 Capped Variance Swaps

The next product I priced and investigated is the capped variance swap. I checked how the different jump parameters affect the price of a capped variance swap compared to the price of a variance swap. In all cases, the cap is fixed at two times the continuous fair variance strike under the Heston model, $C = 2K_{var}^{Hest}$. The simulation is done by the Bates dynamics with the calibrated Heston parameters (with those which violate the Feller-condition) and with severally specified jump parameters.

In the first case I examined the effect of jump intensity. I assumed that the relative jump sizes follow log-normal distribution, with $\mu_J = 0$ expectation and $v_J = 0.1$ standard deviation. λ gets its values from the $[0, 10]$ interval.

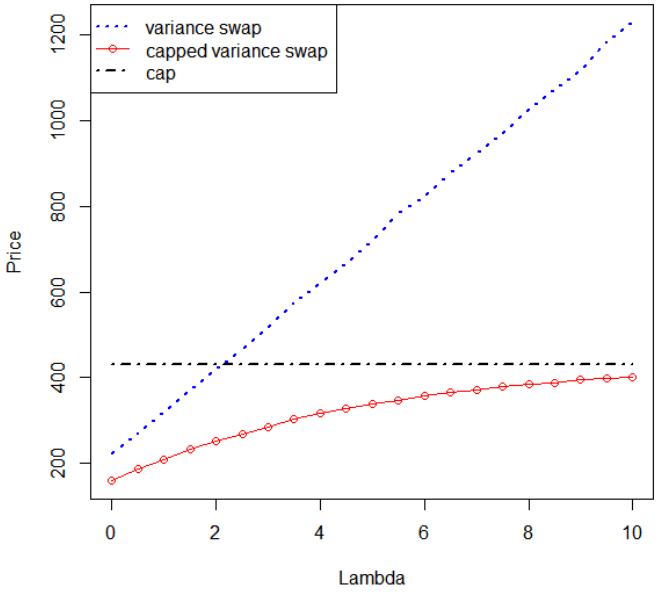

FIGURE 5.12: The price of a variance swap and a capped variance swap as a function of λ.

It can be concluded from figure 5.12 that while the price of the variance swap tends towards infinity as the contribution of jumps gets higher, the price of a capped variance swap approaches the cap's value. It is also clear by this plot, that the variance swap's price is a linear function of the jump intensity.

On the basis of formula 3.13, we expect similar effects on the price caused by the two other jump parameters (μ_J and v_J) since the fair continuous variance strike depends on their squared values. The only difference is the domain of the parameters: $\mu_J \in \mathbb{R}$ but $v_J \in \mathbb{R}^+$ only. On the following two plots $\lambda = 50$ and one of the two other parameters is fixed at 0.[11] Firstly, on figure 5.13, μ_J varies from -0.04 to 0.04 while $v_J = 0$. Conversely, on figure 5.14, μ_J is fixed at zero and $v_J \in [0, 0.05]$

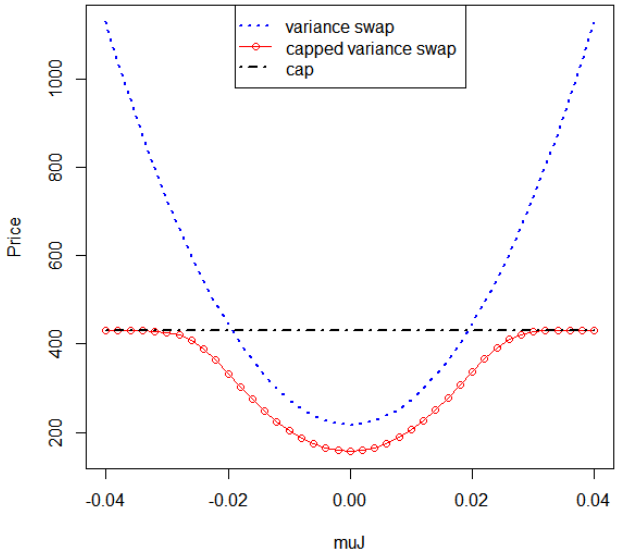

FIGURE 5.13: The price of a variance swap and a capped variance swap as a function of μ_J.

The similarity of the parameters' effects and the squared dependence of the price appear on figures 5.13 and 5.14. It is also important to note that the price of the capped variance swap (with these parameters) is always below the corresponding variance swap's. This follows from the structure of the capped variance swap's payoff and the realized, simulated values. If the cap was higher, or the simulated values were lower (and therefore the cap exceeded the realized variances on all paths) the price of the capped variance swap would be equal to the price of the corresponding variance swap.

[11] These parameters were chosen to get reasonable figures. When λ is small, one of the two other (or both) jump parameters should be large in order to get the jumps' contribution big enough. If the total impact of jumps is mainly caused by μ_J or v_J, the value of the variance swap rises faster due to the squared dependence. Therefore, fixing λ at a greater value and μ_J (or v_J) at zero is a better way to illustrate the effect of v_J (or μ_J, respectively).

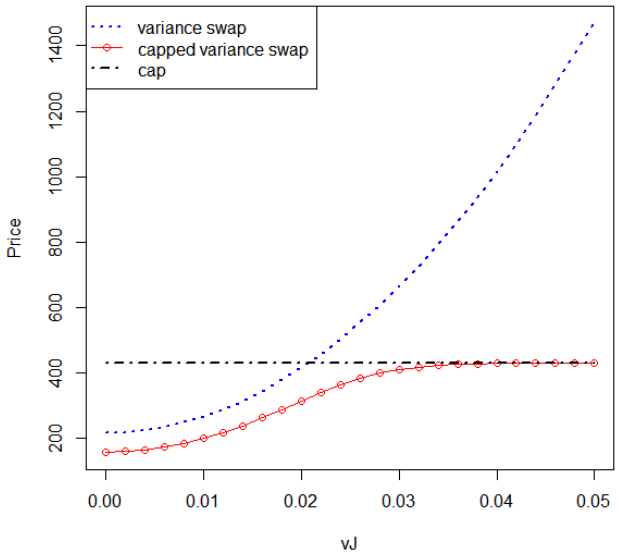

FIGURE 5.14: The price of a variance swap and a capped variance swap as a function of v_J.

I examined the price of a capped variance swap in a different way. All of the model parameters were fixed (both the calibrated Heston and Bates parameters were used separately) but the value of the cap changed. We expect the price of the capped variance swap to tend to the variance swap's price as the cap's value increases. A greater cap yields less paths on which the realized variance exceeds the cap's value and therefore the capped variance swap captures a greater slice of the realized variance.

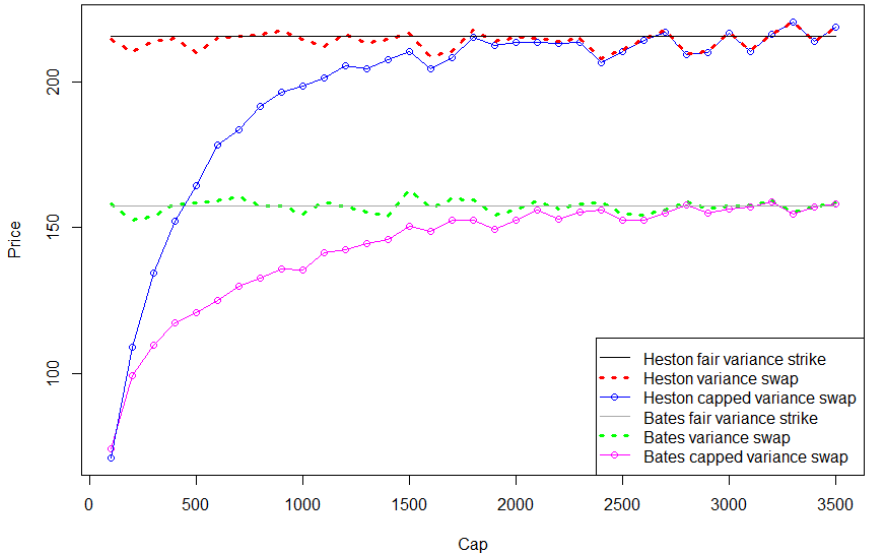

FIGURE 5.15: The price of the capped variance swap converges to the price of the variance swap as the cap increases.

Figure 5.15 presents this feature of capped variance swap. For larger caps the two prices (the prices of variance and capped variance swaps under the selected models, individually)

are identical. A consequence of this is that the capped variance swap's price is always upper bounded by the price of the corresponding variance swap (and obviously by the cap as well). Remark that, since it is the result of different simulations for all caps, the simulated variance strikes are not the same as the fair strike under the Heston nor the Bates model but are close to that value. On this plot we can also compare the prices of these derivatives under the two calibrated models. The prices obtained from the Heston dynamics are higher than the corresponding values under the Bates model. Furthermore, it looks as if the prices of capped variance swaps converge a little bit faster to the simulated variance strikes (as the cap increases) under the Heston model than in the case of Bates model.

5.3.2.3 Corridor Variance Swaps

Firstly, in this section I analyzed the effect of jumps on a down corridor variance swap via the jump parameters. In all cases the upper barrier is fixed at $U = 2700$. Similarly to the previous products, for this test, the Bates dynamics were used along with the calibrated Heston parameters. The jump parameters were defined separately for all cases. To begin with the observation of the effect of λ, the two other parameters were set to $\mu_J = 0$ and $v_J = 0.1$. λ runs from 0 to 1.5.

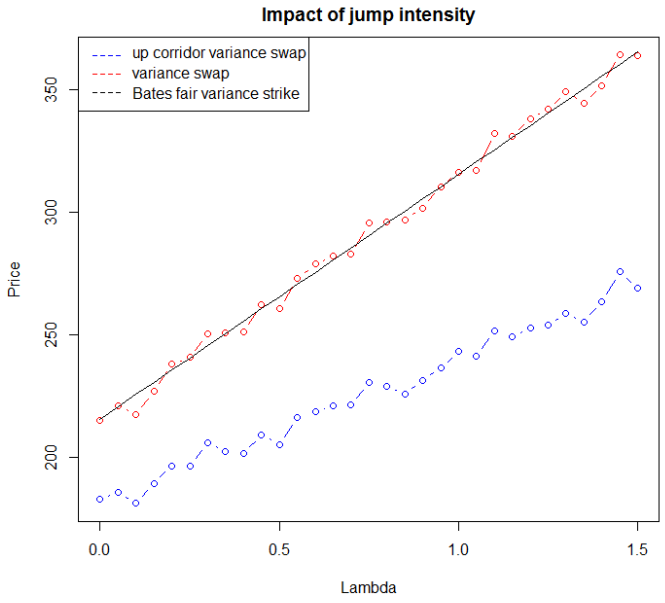

FIGURE 5.16: The price of a variance swap and a down corridor variance swap as a function of λ.

The results are plotted on figure 5.16. Alike to the previous results the simulated variance strikes are dispersed around the fair Bates strikes. As λ increases the difference between the value of the corridor and the variance swap increases as well. Since a corridor swap

always worth less than the corresponding variance swap, it follows that the fair strike of the corridor swap also[12] increases linearly with the jump intensity but with a smaller coefficient of gradient than the variance swap. It explains the greater differences for greater λ-s.

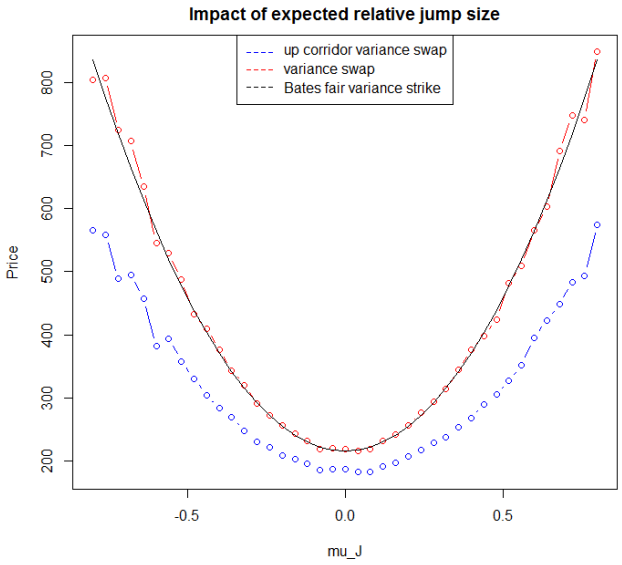

FIGURE 5.17: The price of a variance swap and a down corridor variance swap as a function of μ_J.

On figure 5.17, μ_J varies from -0.8 to 0.8, $\lambda = 0.09703$ and $v_J = 0$. In this case, the symmetry, the lower values of the corridor swap and the greater differences between the two derivatives' prices on the edges can be observed as well.

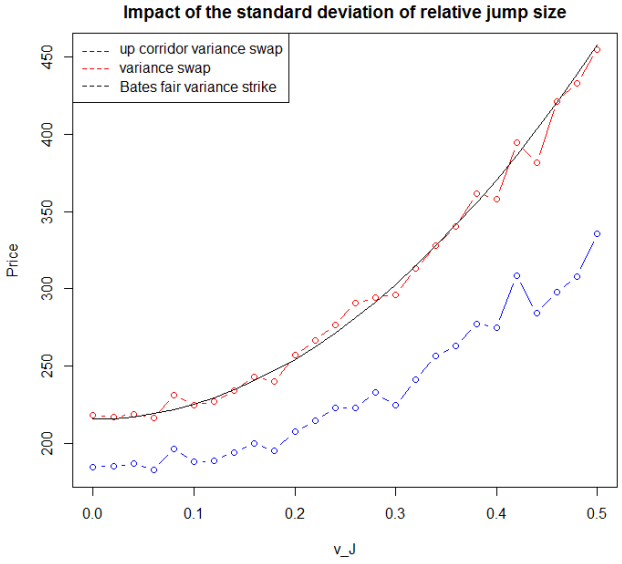

FIGURE 5.18: The price of a variance swap and a down corridor variance swap as a function of v_J.

[12]This feature of variance swaps can be seen from the formula of the fair strike under the Bates model, eq. (3.13).

The effect of jumps regarding the standard deviation of jump sizes, v_J are plotted on figure 5.18. The fixed parameters are $\lambda = 0.09703$, $\mu_J = 0$ and the variable $v_J \in [0, 0.5]$. Again, the lower values of the corridor swap and the increasing differencies between the prices are perceptible.

I also examined the effect of differently chosen corridors on the price of corridor variance swaps. For the simulation, both the calibrated Heston and Bates parameters were used.

First, I priced an up corridor variance swap. In this case, each return contributes to the overall variance only if the asset's price (at the actual interval) exceeds the predefined lower bound, L. Therefore, less variance is captured by an up corridor swap than the actually realized amount, so that the price of an up corridor swap should be lower than the corresponding variance swap's. On the following graph, the lower barrier varies from 1500 to 3000 by step size 50.

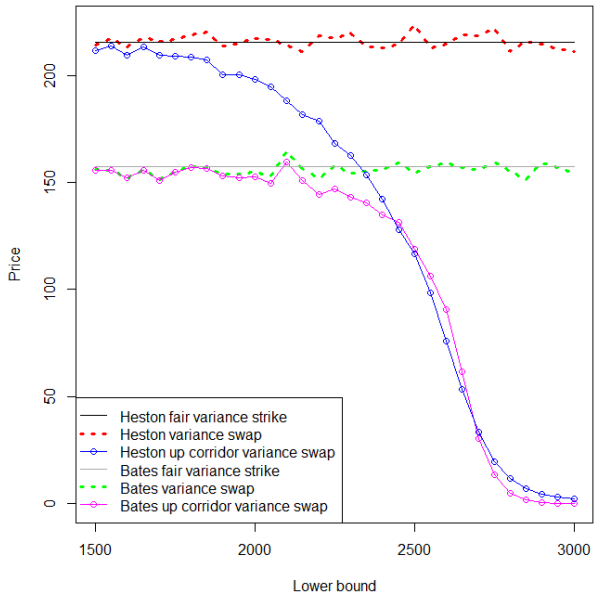

FIGURE 5.19: The price of the up corridor variance swap tends to zero as the the lower barrier increases, $1500 \leq L \leq 3000$.

On figure 5.19 we can see that for small lower bounds the prices of the variance and corridor swaps under the Bates model are identical since the total variance is captured by the up corridor swap. Regarding the Heston model, we would need lower bounds to obtain same prices for the up corridor and the variance swaps. If we increase the value of the barrier, the underlying's price won't be greater than the lower bound on as many paths as it is for smaller values. This results in less variance capturing which implies lower prices. Although, for smaller lower corridors the prices of variance and corridor swaps are greater under the Heston model than under the Bates model, there is a range of lower barrier values when the obtained values under the Bates model for the down corridor swap are greater. This is because the prices of the up corridor variance swap

tend to zero faster, i.e. the curve of its price is steeper than the same curve under the Heston model.

The next product I dealt with is the down corridor variance swap. Its structure is very similar to an up corridor swap's but with an upper barrier, U. It is like the supplementary of an up corridor swap with the same lower bound as the upper bound of the down corridor variance swap, $L = U$. The realized return on the actual interval contributes to the variance captured by a down corridor swap if and only if the asset's spot price is below the upper barrier, $S < U$ which means that it cannot be added to the up corridor swap's payoff. As a consequence, the portfolio of an up corridor and a down corridor variance swaps with the same bounds ($U = L$) captures the total realized variance such as a variance swap.

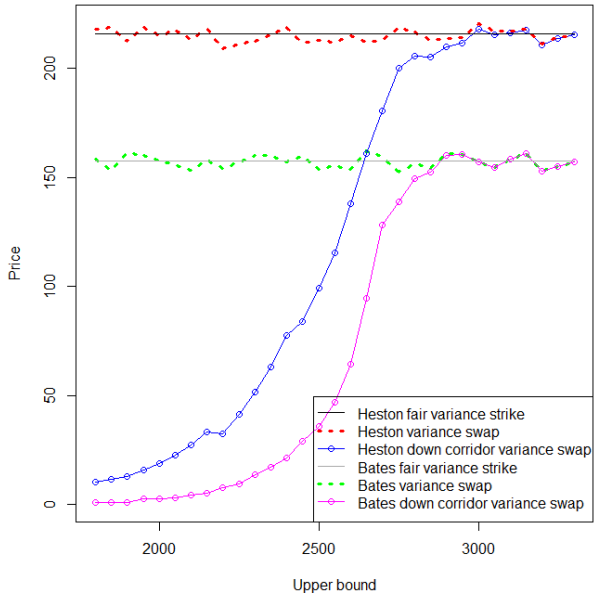

FIGURE 5.20: The price of the down corridor variance swap converges to the price of the corresponding variance swap as the upper barrier increases, $1800 \leq U \leq 3300$.

Figure 5.20 shows the simulated prices of a down corridor and a variance swaps under the Heston and the Bates model for different upper bounds. This figure is similar to the reflection of graph 5.19. The differences arise from the not identical corridor ranges and the randomness of the simulations. An other deviation is the always greater values of the down corridor swap under the Heston model. However, the steeper price curve under the Bates model can be observed as well.

Finally, I investigated how the spot price, S_0 affects the prices of a down corridor and a capped variance swaps under both the Heston and the Bates model.

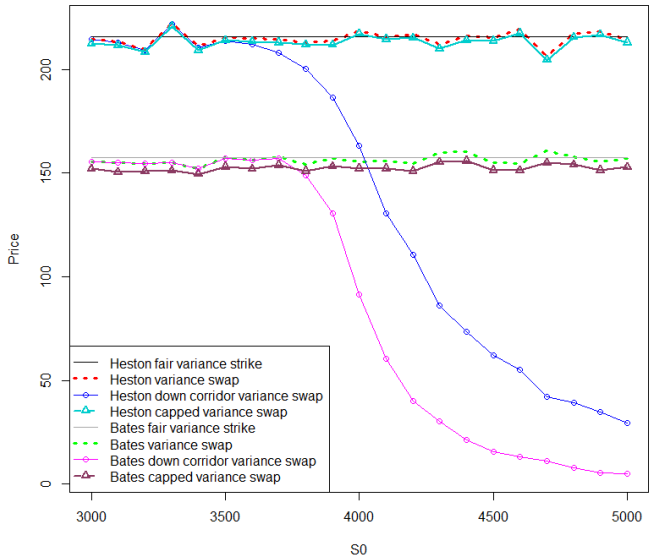

FIGURE 5.21: The prices of a capped and a down corridor variance swaps under the Heston and the Bates model as a function of the asset's spot price. The cap is fixed at 2000 and the upper corridor is $U = 4000$. S_0 varies from 3000 to 5000.

On the basis of figure 5.21, we can state that the fair strike of the capped variance swap is insensitive to the spot price movements. This also follows from the structure of its payoff: it does not depend on S_0. An other remark is about the shape of the down corridor swap's value as a function of S_0: it looks like the up corridor swap's value as an increasing function of its lower barrier L. A down corridor swap captures the realized variance if $S_{i-1} < U$. This means that if the spot price is greater, the prices will be higher on average, and therefore for a fixed upper bound, the capture variance decreases as the spot price increases.

Chapter 6

Conclusion

The aim of this thesis was to demonstrate and analyze some derivatives which are suitable for trading the realized variance effectively. Further goal was to examine the effect of jumps on these derivatives by pricing under two different models: under the Heston model which is a continuous model and under its extension with jumps, the Bates model.

I presented some volatility and variance based derivatives. For gamma, corridor and variance swaps I introduced their replicating portfolio.

Then, I calibrated the Heston and the Bates models to market data. In the case of the Heston model, the calibration wasn't successful as long as the parameters of the model were forced to satisfy the Feller condition. After easing this restriction, a better fit was achieved. Although these calibration results are not perfect, the obtained parameters were suitable for the purpose. Moreover, the calibrations seemed quite stable.

I also estimated the prices of variance and gamma swaps by their replicating portfolio. The obtained strike of a variance swap - using only the available option prices - turned out to be lower than the fair strike under the Heston model which is one limitation of the model-independent replication. The fair model-independent price of a variance swap was compared to the price under the Heston model, since both frameworks assume diffusive price dynamics.

The effects of jumps by the different parameters on the price of variance swaps (and on the other variance based derivatives as well) showed consistent results with the fair formulas of variance strikes under the Bates model would imply.

Finally, I compared the prices of variance swaps with additional features, for example with caps or with corridors, under the Heston and the Bates model. These products exhibited those traits which were expected on the basis of their payoff.

Bibliography

[1] Andersen, L. (2007) *Efficient Simulation of the Heston Stochastic Volatility Model*, Banc of America Securities

[2] Bates, D.S. (1996) *Jumps and Stochastic Volatility: Exchange Rate Processes Implicit in Deutsche Market Options*, University of Pennsylvania and National Bureau of Economic Research

[3] Broadie, M., Jain, A. (2008) *The Effect of Jumps and Discrete Sampling on Volatility and Variance Swaps*, International Journal of Theoretical and Applied Finance, Vol.11, No.8. 761-797.

[4] Capped Variance Swaps, <https://www.fincad.com/resources/resource-library/article/capped-variance-swaps>

[5] Carr, P., Madan, D. (2002) *Towards a Theory of Volatility Trading*

[6] Carr, P., Roger, L. (2009) *Robust Replication of Volatility Derivatives*

[7] Cox, J.C., Ingersoll, J.E., Ross, S.A. (1985) *A Theory of the Term Structure of Interest Rates*, Econometrica, Vol. 53, No. 2 (Mar., 1985), pp. 385-407

[8] Crosby, J., Davis, M. H. A. (2011) *Variance Derivatives: Pricing and Convergence*

[9] Demeterfi, K., Derman, E., Kamal, M., Zou, J. (1999) *More Than You Ever Wanted To Know*[1] *About Volatility Swaps*, Goldman Sachs, Quantitative Strategies Research Notes

[10] Klebaner, F. C. (2005) *Introduction to Stochastic Calculus With Applications*, Imperial College Press

[11] Gatheral, J. (2004) *A parsimonious arbitrage-free implied volatility parameterization with application to the valuation of volatility derivatives*, Global Derivatives & Risk Management 2004

[12] Härdle, W.K., Silyakova, E. (2011) *Variance Swaps*

[1] But Less Than Can Be Said

[13] Heston, S. L. (1993) *A Closed-Form Solution for Options with Stochastic Volatility with Applications to Bond and Currency Options* Yale University

[14] Mougeot, N. (2005) *Volatility Investing Handbook*, BNP Paribas, Equity and Derivatives Research

[15] Overhaus, M., Bermudez, A., Buehler, H., Ferraris, A. Jordinson, C., Lamnouar, A. (2007) *Equity Hybrid Derivatives*, Wiley Finance Series.

[16] Rouah, F. (2013) *The Heston Model and Its Extensions in Matlab and C#*, Wiley Finance Series.

[17] VIX Options and Futures <http://www.cboe.com/products/vix-index-volatility/vix-options-and-futures>

[18] Yuen, C. H., Zheng, W., Kwok, K. K. (2015) *Pricing Exotic Discrete Variance Swaps under the 3/2 Stochastic Volatility Models*

[19] Zhao, H., Zhao, Z., Chatterjee, R., Lonon, T., Florescu, I. (2017) *Pricing Variance, Gamma and Corridor Swaps Using Multinomial Trees*

[20] Zheng, W., Kwok, K. K. (2011) *Closed Form Pricing Formulas for Discretely Sampled Generalized Variance Swaps*